STUDY OF EBULLATED BED FLUID DYNAMICS FOR H-COAL. QUARTERLY PROGRESS REPORT NO. 4, SEPTEMBER 1--NOVEMBER 30, 1978

AMOCO OIL CO., NAPERVILLE, IL. RESEARCH AND DEVELOPMENT DEPT

DEC 1978

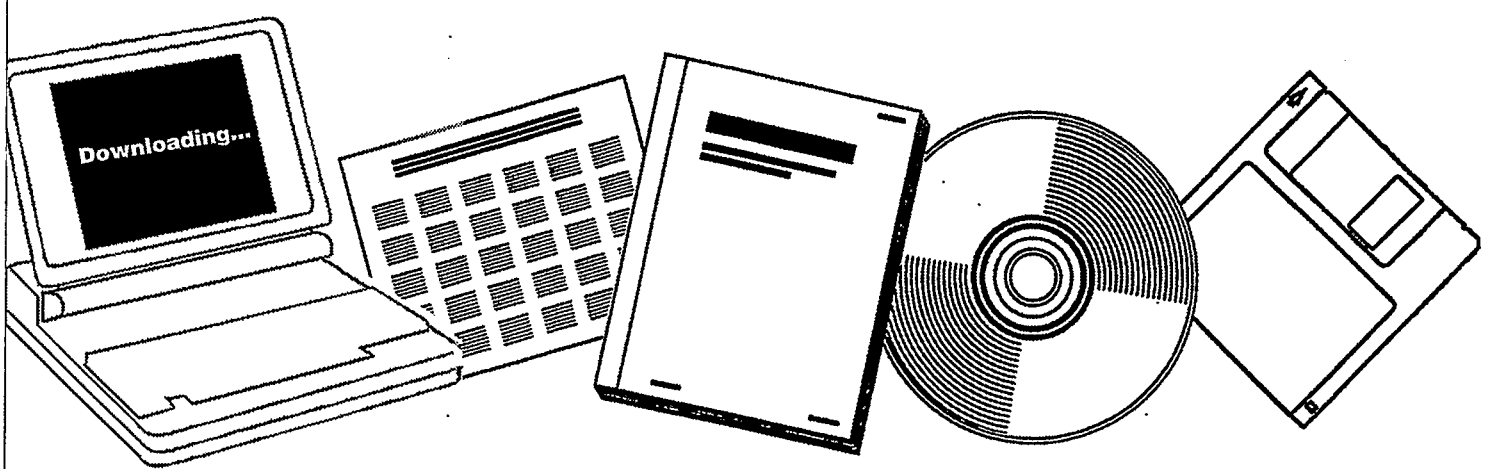

One Source. One Search. One Solution.

NTIS

Providing Permanent, Easy Access to U.S. Government Information

National Technical Information Service is the nation's largest repository and disseminator of government-initiated scientific, technical, engineering, and related business information. The NTIS collection includes almost 3,000,000 information products in a variety of formats: electronic download, online access, CD-ROM, magnetic tape, diskette, multimedia, microfiche and paper.

Search the NTIS Database from 1990 forward

NTIS has upgraded its bibliographic database system and has made all entries since 1990 searchable on **www.ntis.gov.** You now have access to information on more than 600,000 government research information products from this web site.

Link to Full Text Documents at Government Web Sites

Because many Government agencies have their most recent reports available on their own web site, we have added links directly to these reports. When available, you will see a link on the right side of the bibliographic screen.

Download Publications (1997 - Present)

NTIS can now provides the full text of reports as downloadable PDF files. This means that when an agency stops maintaining a report on the web, NTIS will offer a downloadable version. There is a nominal fee for each download for most publications.

For more information visit our website:

www.ntis.gov

U.S. DEPARTMENT OF COMMERCE
Technology Administration
National Technical Information Service
Springfield, VA 22161

FE-2588-15
Distribution Category UC-90d

FE258815

STUDY OF EBULLATED BED FLUID DYNAMICS FOR H-COAL

QUARTERLY PROGRESS REPORT NO. 4
SEPTEMBER 1-NOVEMBER 30, 1978

I. A. VASALOS, E. M. BILD, D. F. TATTERSON

DATE PUBLISHED: DECEMBER, 1978

CONTRACT EF-77-C-01-2588

Research and Development Department

Amoco Oil Company
P. O. Box 400
Naperville, Illinois
60540

Page Intentionally Left Blank

TABLE OF CONTENTS

		Page
FOREWORD		5
OBJECTIVES AND SCOPE OF WORK		6
SUMMARY OF PROGRESS TO DATE		6
	Unit Modification	6
	Data Collection	6
	Costs	7
CONSTRUCTION OF COLD FLOW UNIT AND DATA COLLECTION		7
	Unit Modifications	7
	Viscosity Measurement	8
	Measurement of the Physical Properties of H-Coal Liquids	8
	Unit Data	8
FUTURE PLANS		12
NOMENCLATURE		13
TABLE I	EXPERIMENTAL TESTS COMPLETED	14
TABLE II	EXPERIMENTAL DATA FROM RUN 201	17
TABLE III	EXPERIMENTAL DATA FROM RUN 203	18
TABLE IV	EXPERIMENTAL DATA FROM RUN 204	19
TABLE V	EXPERIMENTAL DATA FROM RUN 205	20
TABLE VI	BED EXPANSION FOR RUN 201: LIQUID KEROSENE, 0% FINES	21
TABLE VII	BED EXPANSION FOR RUN 203: LIQUID KEROSENE, 1% FINES	22
TABLE VIII	BED EXPANSION FOR RUN 204: LIQUID KEROSENE, 5% FINES	23
TABLE IX	BED EXPANSION FOR RUN 205: LIQUID KEROSENE, 10% FINES	24
TABLE X	CALCULATED HOLDUPS IN CATALYST DENSE PHASE FOR THREE-PHASE TESTS, RUN 201	25
TABLE XI	CALCULATED HOLDUPS IN CATALYST DENSE PHASE FOR RUN 201	26
TABLE XII	CALCULATED HOLDUPS IN CATALYST DENSE PHASE FOR RUN 203	27
TABLE XIII	CALCULATED HOLDUPS IN CATALYST DENSE PHASE FOR RUN 204	28
TABLE XIV	CALCULATED HOLDUPS IN CATALYST DENSE PHASE FOR RUN 205	29
TABLE XV	RICHARDSON-ZAKI INDEX FOR RUNS 203, 204, AND 205	30
TABLE XVI	DISTRIBUTION OF COAL CHAR IN REACTOR RUNS 204 AND 205	31
TABLE XVII	TEST CONDITIONS FOR A-41 RADIOTRACER TESTS	32
TABLE XVIII	RADIOACTIVE GAS TRACER TEST DATA	33
TABLE XIX	CALCULATED GAS HOLDUPS FROM GAS RADIOACTIVE TRACER TESTS	34

TABLE OF CONTENTS
-2-

		Page
Figure 1	% BED EXPANSION VS. U_g; RUN 201, KEROSENE/0% FINES	35
Figure 2	% BED EXPANSION VS. U_g; RUN 203, KEROSENE/1% FINES	36
Figure 3	% BED EXPANSION VS. U_g; RUN 204, KEROSENE/5% FINES	37
Figure 4	% BED EXPANSION VS. U_g; RUN 205, KEROSENE/10% FINES	38
Figure 5	CATALYST HOLDUP VS. U_g; RUN 201, KEROSENE	39
Figure 6	CATALYST HOLDUP VS. U_g; RUN 204, KEROSENE + 5 VOL% COAL CHAR	40
Figure 7	CATALYST HOLDUP VS. U_g; RUN 205, KEROSENE + 10 VOL% COAL CHAR	41
Figure 8	BED VOIDAGE VS. U_l/U_t, RUN 201	42
Figure 9	BED VOIDAGE VS. SUPERFICIAL LIQUID VELOCITY, RUN 203	43
Figure 10	BED VOIDAGE VS. SUPERFICIAL LIQUID VELOCITY, RUN 204	44
Figure 11	BED VOIDAGE VS. SUPERFICIAL LIQUID VELOCITY, RUN 205	45
Figure 12	BED VOIDAGE VS. U_l/U_t, RUN 203	46
Figure 13	BED VOIDAGE VS. U_l/U_t, RUN 204	47
Figure 14	BED VOIDAGE VS. U_l/U_t, RUN 205	48
Figure 15	DRIFT FLUX VS. GAS HOLDUP, RUN 201	49
Figure 16	DRIFT FLUX VS. GAS HOLDUP, RUNS 203 AND 204	50
Figure 17	DRIFT FLUX VS. GAS HOLDUP, RUN 205	51
Figure 18	RADIOTRACER DETECTOR LOCATION: H-COAL FLUID DYNAMICS FLOW SHEET	52
Figure 19	RECORDER TRACER INJECTION OUTPUT, TEST 9	53
Figure 20	INTERNAL AGE AND INTENSITY FUNCTION VS. TIME; TEST 4	55
Figure 21	INTERNAL AGE AND INTENSITY FUNCTION VS. TIME; TEST 6	56
Figure 22	INTERNAL AGE AND INTENSITY FUNCTION VS. TIME; TEST 8	57
Figure 23	INTERNAL AGE AND INTENSITY FUNCTION VS. TIME; TEST 10	58

FOREWORD

The H-Coal process, developed by Hydrocarbon Research, Incorporated (HRI), involves the direct catalytic hydroliquefaction of coal to low-sulfur boiler fuel or synthetic crude oil. The 200-600 ton-per-day H-Coal pilot plant is being constructed next to the Ashland Oil, Incorporated refinery at Catlettsburg, Kentucky under ERDA contract to Ashland Synthetic Fuels, Incorporated. The H-Coal ebullated bed reactor contains at least four discrete components: gas, liquid, catalyst, and unconverted coal and ash. Because of the complexity created by these four components, it is desirable to understand the fluid dynamics of the system. The objective of this program is to establish the dependence of the ebullated bed fluid dynamics on process parameters. This will permit improved control of the ebullated bed reactor.

The work to be performed is divided into three parts: review of prior work, cold flow model construction and operation, and mathematical modeling. The review of prior work has been completed. The objective of this quarterly progress report is to outline progress in the second part during the fifth quarter of the project.

OBJECTIVES AND SCOPE OF WORK

The overall objective of this project is to improve the control of the H-Coal reactor through a better understanding of the hydrodynamics of ebullated beds. The project is divided into three main tasks:

1) Review of prior work in three-phase fluidization.

2) Construction of a cold flow unit and collection of data.

3) Development of a mathematical model to describe the behavior of gas/liquid fluidized beds. The model will be based on information available in the literature and on data generated in the cold flow unit.

Progress on Part 1 has already been reported in previous reports. Progress made on Parts 2 and 3 during this quarter is presented in this quarterly status report.

SUMMARY OF PROGRESS TO DATE

Unit Modification

Experiments with kerosene/coal char slurries at concentrations up to 10 vol% continued this period. At coal char concentrations over 5 vol%, continuous operation of the fresh feed and recycle centrifugal pumps was desirable to avoid settling and plugging of the lines and valves. For these reasons, larger motors were installed to avoid pump overheating. In spite of these changes, the pumps did not operate satisfactorily at high gas velocities because they became vapor-locked. A new rotary positive displacement pump was ordered to allow smoother operation at high gas rates.

Data Collection

Completed several important experiments with kerosene, nitrogen, and HDS-2A catalyst (3/16" in length, 1/16" in diameter) with coal char concentrations of 0, 1, 5, and 10 vol%. In each case the bed expansion is defined by scanning the entire reactor length with a computer-operated gamma-ray elevator. Data obtained at different operating conditions were correlated using correlations identified during the literature search. The liquid/slurry catalyst expansion data were correlated using the Richardson-Zaki equation. This defines the volume fraction occupied by the liquid as an n^{th} power function of the ratio of the liquid superficial velocity to the particle terminal velocity. It was found that the power n increases with the concentration of the coal char particles. The gas/slurry/catalyst data were correlated using the drift flux

correlation developed by Darton and Harrison. It was found that with kerosene slurries the gas is distributed in uniform bubbles at coal char concentrations up to 10 vol% and low gas and liquid velocities. At higher velocities and coal char concentrations, the gas bubbles coalesce into bigger bubbles, resulting in an unstable bed operation. Additional data were also obtained this quarter by using Argon-41 radioactive tracer to find out the gas residence time in the reactor. Results from these experiments are discussed in this report.

Costs

By the end of the third quarter, about $489,000 was committed to the project. Future projections indicate that no cost overruns are anticipated at this time.

CONSTRUCTION OF COLD FLOW UNIT AND DATA COLLECTION

Unit Modifications

Several tests were conducted with kerosene and coal char slurries at concentrations of 1,5 and 10 vol%. At coal char concentrations over 5 vol%, continuous operation of the fresh feed and recycle centrifugal pumps was desirable to avoid settling and plugging of the lines and valves. For this reason, new 1.5 HP motors were installed on the feed and recycle pumps. Continuous pump operation with coal slurries had caused the existing 0.75 HP motors to overheat. Improved operation has been observed with the new motors. It has also been found that plugging problems are not as severe with kerosene/coal char as it was earlier in the program with water/coal char slurries. This may also be a factor in preventing pump overheating with the larger motors and kerosene slurries.

Another change in the pumps includes the replacement of the stainless steel washers with ceramic washers. Stainless steel washers in the pumps were wearing very rapidly. Although it has been found that ceramic washers do not wear, they tend to fracture. For this reason, tungsten carbide washers were ordered.

The modified centrifugal pumps are performing well provided that the amount of gas entrained in the recycle line is not excessive. It was found that under certain conditions the centrifugal pump becomes vapor-locked. A Tuthill rotary positive displacement pump was ordered to replace the existing recycle pump. This will handle a much higher concentration of entrained gas.

Another unit modification involved the measurement of the differential pressures along the reactor. Currently, four gas-purged impulse lines enter the reactor through the spool pieces located about five feet apart. Continuous gas purging reduces the problems of line plugging at the high coal char concentrations.

Data Collection

Viscosity Measurement.--A capillary tube viscometer described in a previous report was used to measure the viscosity of a 1 vol% coal char/kerosene slurry. The viscosity was determined to be 1.36 cp at 74°F; the viscosity of kerosene is 1.39 at 70°F.

Use of higher concentration kerosene slurries and mineral oil slurries caused the capillary tube to plug. A new capillary tube viscometer was constructed which has a 0.356 cm ID compared with a 0.155 cm ID of the previous viscometer. Viscosity measurements were continued with the larger viscometer.

A 5 vol% coal char/kerosene slurry was tested. However, with the larger diameter viscometer, the flow was turbulent, so the results could not be used. A 10 vol% coal char/kerosene slurry will be tested. With the higher viscosity, the flow may revert to laminar and the Hagen-Poiseuille equation will be applicable.

Measurement of the Physical Properties of H-Coal Liquids.--No samples were obtained from the PDU for viscosity measurement. Other higher priority PDU work necessitated the postponement of these samples to a later date. For this reasons, the contract with Battelle was extended six months.

Unit Data.--Experiments were conducted with HDS-2A catalyst 3/16" in length and 1/16" in diameter. The catalyst was fluidized with liquid kerosene slurries up to 10 vol% coal char. Nitrogen gas was also used in most of the runs. Experimental test conditions for the runs carried out this quarter are shown in Table I. A summary is reported below:

Run No.	Fines, Vol%	Test No.	Liquid Flow Rate, GPM/Ft^2	Gas Flow Rate, Ft/Sec
201	0	9-44	22-89	0-0.25
203	1	1-11	22-89	0-0.20
204	5	1-28	31-82	0-0.15
205	10	9-34	38-90	0-0.25

For each test, a gamma-ray scan was used to determine the catalyst bed height. As reported in previous reports, a Cs-137 source is used in conjunction with a NaI crystal scintillation counter. This counter monitors the amount of γ-rays not absorbed by the reactor liquid slurry or liquid/catalyst mixture. The bed interface is detected by the sharp difference in the number of counts which exists in most of the cases between the bed and the dilute phase above it.

The bed height thus determined and the number of counts per second (cps) below and above the bed for all tests carried out this quarter are reported in Tables II, III, IV, and V. From the bed height at each condition and the settled bed height (no flow), the per cent bed expansion was calculated and shown in Tables VI to IX. Plots of per cent bed

expansion vs. gas velocity (U_g) with liquid velocity (U_l) as a parameter are shown in Figures 1 to 4 for Runs 201, 203, 204, and 205, respectively. To calculate bed expansion, the zero bed height is remeasured prior to each new test. Due to catalyst attrition and carryover, the bed level changes with time. The zero height reported in the tables was the initial bed height, but with catalyst losses and the addition of small amounts of catalyst, this zero cannot be used to calculate per cent bed expansion. For example, large errors would result from using the reported initial bed height to calculate bed expansion for Run 201. This results because of several changes in bed height over the time in which these tests were run.

For Run 201 at U_l = 0.05 ft/sec, the bed expansion initially decreases with the addition of gas. This anomaly may result because the liquid flow rate is below the minimum fluidization velocity. For Runs 203 and 204, per cent bed expansion always increased with an increase in gas velocity. With the 10 vol% coal char/kerosene slurry, Run 205, at liquid velocities of 0.085 and 0.10 ft/sec, the bed expansion decreased when the gas velocity increased over 0.10 ft/sec. The bed expansion continued to decrease up to a gas velocity of 0.25 ft/sec.

The bed contraction has been documented by numerous investigators as reviewed in the Amoco literature search. Bed contraction occurs because liquid entrained in gas bubble wakes passes through the bed at a greater velocity than the rest of the liquid, depleting the bed of liquid. The loss of liquid causes the catalyst bed to contract.

Bed expansion increased as coal char was added to the kerosene. At the liquid superficial velocity of 0.20 ft/sec, the bed expansion increased from about 76% to 116% for kerosene when 10 vol% coal char was added. These are much greater bed expansions than those found in the PDU.

Phase holdups calculated from gamma-ray scan and bed height measurements are given in Tables X through XIV. Plots of ϵ_c vs. U_g with U_l as a parameter are shown in Figures 5, 6, and 7 for Runs 201, 204, and 205. Bed contraction with the addition of gas can also be seen with these plots.

For Runs 201 and 204, ϵ_c generally decreased with increasing liquid and gas flow rates. However, for Run 205 with 10 vol% coal char added to the kerosene, ϵ_c increased for two liquid velocities when U_g increased over 0.10 ft/sec. Again, this indicates that, following initial bed expansion, the catalyst bed can decrease with an increase in gas flow.

Liquid/catalyst holdup data were analyzed with the Richardson-Zaki correlation. This correlation relates liquid holdup to liquid velocity:

$$\epsilon_l^n = U_l/U_t$$

A plot of ϵ_l vs. U_l/U_t for Run 201 is shown in Figure 8. The additional tests performed this quarter are shown with data previously obtained. The Richardson-Zaki index, n, determined from the slope of the line is 2.9.

Plots of ϵ_l vs. U_l for 1, 5, and 10 vol% coal slurries are shown in Figures 9-11. The plots of ϵ_l vs. U_l/U_t for these runs are given in Figures 12-14. The Richardson-Zaki indices for all runs are given in Table XV.

As expected, n increases with the addition of coal char. Coal char increases the effective viscosity of the slurry and the Richardson-Zaki index is inversely related to the Reynolds number. The addition of 1 vol% coal char should have minimal effect on slurry properties; therefore, the difference between the indices found for Runs 201 and 203 is an indication of the error in determining the index.

Gas/liquid/catalyst data were analyzed with the Darton-Harrison drift flux method. The drift flux, V_{CD},

$$V_{CD} = U_g(1 - \epsilon_g) - \frac{U_l(1 - \epsilon_g)\epsilon_g}{\epsilon_l}$$

is plotted vs. gas holdup. Flow transitions can be identified on these plots. Figures 15, 16, and 17 show these plots for Runs 201, 203, 204, and 205. Lines showing the uniform-bubbly and churn-turbulent flow regimes for water are given for comparison. The slope of the line defining ideal or uniform-bubbly flow for kerosene has a smaller slope than the line defining bubbly flow for water. This indicates the slope of the line may be related to the particle Reynolds number, which is lower for kerosene than for water.

The transition from uniform-bubbly to churn-turbulent flow did not occur for kerosene or kerosene with up to 5 vol% coal char systems. When 10 vol% coal char was added to the kerosene, the flow regime made a transition from bubbly to churn-turbulent. This indicates an increase in viscosity favors bubble coalescence, creating larger bubbles causing the flow transition to churn-turbulent. The effect of increasing viscosity favoring bubble coalescence has already been noted for gas/liquid systems.

For the water system, transition from uniform-bubbly to churn-turbulent occurred for all water and water/coal char slurry systems. For kerosene, the transition occurred only when 10 vol% coal char was added. The lower surface tension of kerosene enhances bubble breakup. Therefore, kerosene systems will tend to remain in the ideal-bubbly flow regime until viscosity effects due to the addition of coal char, become dominant. Uniform-bubbly flow is the preferred flow regime for the H-Coal reactor because of the greater flow stability.

To determine the coal char distribution in the reactor, samples were taken. The results from these samples are shown in Table XVI for Runs 204 and 205. In both cases there is an indication that the coal char concentration increases toward the top of the reactor. Particle size analysis of the coal char samples is also being performed to determine if the coal is segregating according to size. The viscosity of the filtrate kerosene was determined to be 1.217 at 100°F.

Radioactive gas tracer tests were conducted this quarter. Argon-41, a radioactive gamma-ray emitter, was injected into the bottom spool piece of the FDU. Its progress through the reactor was monitored using externally mounted NaI scintillation crystal detectors. The location of the detectors on the unit is shown in Figure 18. Sixteen injections of tracer were made into the column; each injection contained about 1.5 millicuries of A-41. The system conditions for each injection are given in Table XVII.

A sample recorder output for Test 9 is shown in Figure 19. The results from Detector 1 could not be used. This detector was next to the injection assembly and saw high levels of radiation at all times. This detector requires more extensive lead shielding to obtain meaningful data at the injection point.

Data from the radioactive tracer tests are reported in Table XVIII. Many of the tests were replicates, and results from only one of the replicates are given.

The first and second moments were determined from the tracer concentration-age curves. The first moment corresponds to the mean residence time, and the second moment corresponds to the variance. However, with trailing time distributions as in this case, large errors in the second moment can occur. Therefore, $m(\theta^2)$ probably is not a good estimate of the variance.

Using the mean residence time at each detector, the linear velocity, $\overline{U}_g$, of the tracer at different points in the reactor can be determined. Using the linear velocity and gas superficial velocity, the gas holdup can be calculated:

$$\epsilon_g = \frac{U_g}{\overline{U}_g}$$

These calculated gas holdups are reported in Table XIX. Gas holdups in the catalyst bed and above the catalyst bed are given. For comparison, results from gamma-ray scans for identical test conditions are also shown.

In general, there is fairly good agreement between tracer results and gamma-ray scan results, except for Test 4. In all cases, the gas holdup determined from the radioactive tracer tests was greater than the gamma-ray scan result. This may result from an effect due to the injection velocity of the tracer. These results indicate the tracer was injected at a lower velocity than the rest of the gas. To avoid this problem, during the next tracer test the radioactive tracer will be injected before the distributor so it will be better mixed with the gas in the reactor.

The internal age distribution and intensity function were also evaluated for each of the tracer tests. The definition of these functions is given below:

$$I_t(+) = \frac{1 - \int_0^t E(t)\,dt}{\bar{t}}$$

$$\lambda(+) = 1/\bar{t}\ \frac{E(t)}{I(t)}$$

where: $I(+)$ = internal age distribution.
$\lambda(+)$ = intensity function.
t = mean residence time.
$E(t)$ = external age distribution (tracer concentration)

Plots of these functions can be used to determine existence of bypassing or dead space in the reactor. Several sample plots for these tests are shown in Figures 20-23.

The internal age distribution plot should be smooth, without any humps, if reactor bypassing is not occurring. In all cases, the plots of internal age distribution indicate there is no bypassing. The intensity function will be monotonically increasing with respect to t if the reactor is free of dead space. However, none of the plots of intensity function is monotonically increasing. This indicates that at a variety of flow conditions, part of the reactor is stagnant. A better test of reactor dead space will be made when the tracer is added through the distributor into the reactor. These plots may be due to poor mixing of tracer in the gas flow rather than dead space in the reactor.

FUTURE PLANS

1) Complete experiments with kerosene/coal char slurries at room temperature. Tests with 15 vol% coal char with N_2 and Freon-12 will be completed.

2) Start experiments with kerosene slurries heated to reduce the viscosity.

3) Perform next radioactive gas tracer test with kerosene.

4) Continue measurement of kerosene/coal slurry viscosity with capillary tube viscometer.

NOMENCLATURE

d	Particle diameter.
d_p	Diameter of a circle of the same area as the projected particle in its most stable position.
d_s	Diameter of a sphere with the same volume as the particle.
D	Bed diameter.
ϵ_{cs}	Catalyst volume fraction from bed height data.
$\epsilon_{c\gamma}$	Catalyst volume fraction from gamma-ray data.
ϵ_g	Gas volume fraction.
$\epsilon_{g\gamma_s}$	Gas volume fraction from bed height and γ-ray data.
ϵ_l	Liquid volume fraction.
$\epsilon_{l\gamma_s}$	Liquid volume fraction from bed height and γ-ray data.
K	Heywood particle shape factor.
n	Richardson-Zaki index.
U_g	Superficial gas velocity.
U_l	Superficial liquid velocity.
U_t	Terminal velocity.
V_{cD}	Gas drift flux.

TABLE I

EXPERIMENTAL TESTS COMPLETED

Run No.	Catalyst	Liquid	Fines, Vol%	Test No.	Liquid Flow Rate, GPM/Ft^2	Gas Flow Rate, Ft/Sec
201	HDS-2A	Kerosene	0.0	-09	83.03	0.0
	L = 3/16"			-10	89.76	0.0
	D = 1/16"			-11	100.5	0.0
				-45	44.88	0.25
203			1.0	-01	22.44	0.0
				-02	44.88	0.0
				-03	67.32	0.0
				-04	89.76	0.0
				-05	22.44	0.05
				-06	22.44	0.20
				-07	44.88	0.05
				-08	44.88	0.15
				-09	67.32	0.05
				-10	67.32	0.10
				-11	89.76	0.05
204			5.0	-01	31.42	0.0
				-02	44.88	0.0
				-03	60.59	0.0
				-04	67.32	0.0
				-05	76.30	0.0
				-06	89.76	0.0
				-07	31.42	0.05
				-08	31.42	0.026
				-09	31.42	0.035
				-10	31.42	0.044
				-11	31.42	0.10
				-12	31.42	0.15
				-14	44.88	0.035
				-15	44.88	0.044
				-16	44.88	0.05
				-17	44.88	0.10
				-18	67.32	0.026
				-19	67.32	0.035
				-20	67.32	0.044
				-21	67.32	0.05
				-22	81.68	0.026
				-23	81.68	0.035
				-24	81.68	0.044
				-25	31.42	0.10
				-26	31.42	0.026
				-27	44.88	0.10
				-28	67.32	0.026
205			10.0	-01	38.15	0.0
				-02	44.88	0.0
				-03	51.61	0.0
				-04	60.59	0.0
				-05	76.30	0.0
				-06	67.32	0.0

TABLE I

EXPERIMENTAL TESTS COMPLETED

-2-

Run No.	Catalyst	Liquid	Fines, Vol%	Test No.	Liquid Flow Rate GPM/Ft	Gas Flow Rate Ft/Sec
201	HDS-2A	Kerosene	0	-12	22.4	0.05
"	L = 3/16"	"	"	-13	22.4	0.026
"	D = 1/16"	"	"	-14	22.4	0.035
"	"	"	"	-15	22.4	0.044
"	"	"	"	-16	22.4	0.077
"	"	"	"	-17	22.4	0.10
"	"	"	"	-18	22.4	0.15
"	"	"	"	-19	22.4	0.20
"	"	"	"	-20	22.4	0.25
"	"	"	"	-21	31.4	0.026
"	"	"	"	-22	31.4	0.035
"	"	"	"	-23	31.4	0.044
"	"	"	"	-24	31.4	0.05
"	"	"	"	-25	31.4	0.077
"	"	"	"	-26	31.4	0.10
"	"	"	"	-27	31.4	0.15
"	"	"	"	-28	31.4	0.20
"	"	"	"	-29	31.4	0.25
"	"	"	"	-30	44.8	0.026
"	"	"	"	-31	44.8	0.035
"	"	"	"	-32	44.8	0.044
"	"	"	"	-33	44.8	0.05
"	"	"	"	-34	44.8	0.077
"	"	"	"	-35	44.8	0.10
"	"	"	"	-36	44.8	0.15
"	"	"	"	-37	44.8	0.20
"	"	"	"	-38	76.3	0.026
"	"	"	"	-39	76.3	0.035
"	"	"	"	-40	76.3	0.044
"	"	"	"	-41	76.3	0.05
"	"	"	"	-42	76.3	0.077
"	"	"	"	-43	67.3	0.10
"	"	"	"	-44	67.3	0.15
205	"	"	10	-09	38.1	0.026
"	"	"	"	-10	38.1	0.035
"	"	"	"	-11	38.1	0.044
"	"	"	"	-12	38.1	0.05
"	"	"	"	-13	38.1	0.077
"	"	"	"	-14	38.1	0.10
"	"	"	"	-15	38.1	0.15

(Table Continued)

TABLE I

EXPERIMENTAL TESTS COMPLETED
-3-

Run No.	Catalyst	Liquid	Fines, Vol%	Test No.	Liquid Flow Rate, GPM/Ft²	Gas Flow Rate, Ft³/Sec
205	HDS-2A,	Kerosene	10	-16	38.1	0.20
"	L = 3/16"	"	"	-17	38.1	0.25
"	D = 1/16"	"	"	-18	44.9	0.026
"	"	"	"	-19	44.9	0.035
"	"	"	"	-20	44.9	0.044
"	"	"	"	-21	44.9	0.05
"	"	"	"	-22	44.9	0.077
"	"	"	"	-23	44.9	0.10
"	"	"	"	-24	44.9	0.15
"	"	"	"	-25	44.9	0.20
"	"	"	"	-26	44.9	0.25
"	"	"	"	-27	67.3	0.026
"	"	"	"	-28	67.3	0.035
"	"	"	"	-29	67.3	0.044
"	"	"	"	-30	67.3	0.05
"	"	"	"	-31	67.3	0.077
"	"	"	"	-32	89.8	0.035
"	"	"	"	-33	89.8	0.044
"	"	"	"	-34	89.8	0.05

EMB/ml
12/20/78

TABLE II

EXPERIMENTAL DATA FROM RUN 201

Test	Catalyst Bed Height (In.)	Gamma-Ray in Bed (CPS)	Gamma-Ray Above Catalyst Level (CPS)
201-12	73.5	249	315
-13	72.0	238	330
-14	78.0	252	317
-15	75.0	250	330
-16	72.6	260	345
-17	72.7	265	355
-18	72.8	270	367
-19	72.9	283	385
-20	73.0	286	392
-21	72.4	229	317
-22	72.4	231	325
-23	78.5	240	337
-24	79.0	241	337
-25	82.5	250	355
-26	86.0	275	376
-27	91.0	285	400
-28	91.0	295	400
-29	92.0	299	405
-30	92.0	236	330
-31	87.0	242	335
-32	88.0	246	335
-33	89.0	250	342
-34	93.0	260	356
-35	95.5	277	375
-36	98.0	301	400
-37	109.5	317	425
-38	117.0	258	330
-39	119.5	264	335
-40	122.3	270	345
-41	122.5	273	350
-42	124.5	291	372
-43	127.5	307	405
-44	123.0	326	446
Zero (Initial)	70.0	--	--
201-09	108.5	244	298
-10	123.6	248	301
-11	133.2	257	300
-45	102.0	314	408

EMB/ml
12/20/78

TABLE III

EXPERIMENTAL DATA FROM RUN 203

Test	Catalyst Bed Height (In.)	Gamma-Ray in Bed (cps)	Gamma-Ray Above Catalyst Level (cps)
Zero (Initial)	69.0	--	--
203-01	69.0	209.4	298.7
-02	79.0	220.4	297.6
-03	101.0	238.0	298.2
-04	115.5	250.0	295.4
-05	77.5	238.0	321.6
-06	82.0	278.0	381.5
-07	83.5	243.0	325.2
-08	97.75	296.0	395.5
-09	106.5	264.9	335.3
-10	119.0	302.0	390.0
-11	124.0	275.0	335.0

TABLE IV

EXPERIMENTAL DATA FROM RUN 204

Test	Catalyst Bed Height (In.)	Gamma-Ray in Bed (cps)	Gamma-Ray Above Catalyst Level (cps)
Zero (Initial)	68.0	-	-
204-01	73.5	214	293
-02	86.3	227	289
-03	101.25	235	292
-04	106.5	238	292
-05	119.5	245	291
-06	133.0	252	291
-07	77.5	234	315
-08	73.1	217	303
-09	74.0	226	305
-10	75.25	237	310
-11	88.0	252	335
-12	87.5	273	355
-14	96.0	248	315
-15	98.0	250	320
-16	105.0	255	325
-17	113.0	295	375
-18	123.5	255	302
-19	125.0	258	315
-20	126.0	269	322
-21	128.25	274	330
-22	138.0	262	308
-23	140.25	270	315
-24	136.75	270	328
-25	83.5	258	342
-26	76.5	227	300
-27	95.9	274	364
-28	113.0	248	308

EMB/ml
11/9/78

TABLE V

EXPERIMENTAL DATA FROM RUN 205

Test	Catalyst Bed Height (In.)	Gamma-Ray in Bed (cps)	Gamma-Ray Above Catalyst Level (cps)
Zero (Initial)	68.0	-	-
205-01	79.0	215	285
-02	86.75	227	283
-03	93.25	225	282
-04	107.5	233	283
-05	130.5	240	280
-06	106.0	245	282
-07	138.0	249	284
-08	147.0	253	283
Zero	67.0	-	-
205-09	80.0	228	298
-10	82.0	230	302
-11	83.0	235	304
-12	86.0	245	310
-13	83.0	250	325
-14	86.0	263	334
-15	85.0	263	343
-16	85.0	259	349
-17	83.0	256	356
-18	89.0	228	289
-19	90.0	236	300
-20	87.0	239	301
-21	89.0	240	305
-22	91.0	252	320
-23	95.0	263	334
-24	94.0	276	338
-25	90.0	259	336
-26	85.0	264	356
-27	114.0	241	287
-28	118.0	245	295
-29	119.0	255	304
-30	120.0	256	310
-31	124.0	278	340
-32	152.0	261	300
-33	153.0	264	305
-34	154.0	271	318

EMB/ml
12/20/78

TABLE VI

BED EXPANSION FOR RUN 201:
LIQUID KEROSENE, 0% FINES

Run No.	Liquid Flow Rate, GPM/Ft²	Gas Flow Rate, Ft/Sec	Catalyst Bed Height, In.	% Bed Expansion
Zero	--	--	70.0	--
201-12	22.4	0.05	73.5	24.0
-13	"	0.026	72.0	21.0
-14	"	0.035	78.0	22.0
-15	"	0.044	75.0	17.0
-16	"	0.077	72.6	14.0
-17	"	0.10	72.7	14.0
-18	"	0.15	72.8	14.0
-19	"	0.20	72.9	14.0
-20	"	0.25	73.0	14.0
-21	31.4	0.026	72.4	14.0
-22	"	0.035	72.4	13.0
-23	"	0.044	78.5	23.0
-24	"	0.05	79.0	24.0
-25	"	0.077	82.5	29.0
-26	"	0.10	86.0	34.0
-27	"	0.15	91.0	42.0
-28	"	0.20	91.0	42.0
-29	"	0.25	92.0	44.0
-30	44.8	0.026	92.0	44.0
-31	"	0.035	87.0	36.0
-32	"	0.044	88.0	38.0
-33	"	0.05	89.0	39.0
-34	"	0.077	93.0	45.0
-35	"	0.10	95.5	49.0
-36	"	0.15	98.0	53.0
-37	"	0.20	109.5	71.0
-38	76.3	0.026	117.0	67.1
-39	"	0.035	119.5	70.7
-40	"	0.044	122.3	74.7
-41	"	0.05	122.5	75.0
-42	"	0.077	124.5	77.8
-43	67.3	0.10	127.5	82.1
-44	"	0.15	123.0	75.7

IAV/ml
12/20/78

TABLE VII

BED EXPANSION FOR RUN 203:
LIQUID KEROSENE, 1% FINES

Run No.	Liquid Flow Rate, GPM/Ft^2	Gas Flow Rate, Ft/Sec	Catalyst Bed Height, Inches	% Bed Expansion
Zero	--	--	69.0	0
203-01	22.44	0	69.0	0
-02	44.88	0	79.0	13
-03	67.33	0	101.0	44
-04	89.76	0	115.5	65
-05	22.44	0.05	77.5	11
-06	22.44	0.20	82.0	17
-07	44.88	0.05	83.5	32
-08	44.88	0.15	97.75	45
-09	67.32	0.05	106.5	58
-10	67.32	0.10	119.0	77
-11	89.76	0.05	124.0	85

IAV/ml
12/20/78

TABLE VIII

BED EXPANSION FOR RUN 204:
LIQUID KEROSENE, 5% FINES

Run No.	Liquid Flow Rate, GPM/Ft^2	Gas Flow Rate, Ft/Sec	Catalyst Bed Height, Inches	% Bed Expansion
Zero	--	--	68.0	-
204-01	31.42	0	73.5	9
-02	44.88	0	86.3	28
-03	60.59	0	101.25	51
-04	67.32	0	106.5	58
-05	76.30	0	119.5	78
-06	89.76	0	133.0	98
-07	31.42	0.05	77.5	15
-08	"	0.026	73.1	9
-09	"	0.035	74.0	10
-10	"	0.044	75.25	12
-11	"	0.10	88.0	31
-12	"	0.15	87.5	30
-14	44.88	0.035	96.0	43
-15	"	0.044	98.0	46
-16	"	0.05	105.0	56
-17	"	0.10	113.0	68
-18	67.32	0.026	123.5	84
-19	"	0.035	125.0	86
-20	"	0.044	126.0	87
-21	"	0.05	128.25	91
-22	81.68	0.026	138.0	105
-23	"	0.035	140.25	109
-24	"	0.044	136.75	103
-25	31.42	0.10	83.5	24
-26	"	0.026	76.5	14
-27	44.88	0.10	95.9	43
-28	67.32	0.026	113.0	68

IAV/ml
12/20/78

TABLE IX

BED EXPANSION FOR RUN 205:
LIQUID KEROSENE, 10% FINES

Run No.	Liquid Flow Rate, GPM/Ft^2	Gas Flow Rate, Ft/Sec	Catalyst Bed Height, Inches	% Bed Expansion
Zero	--	--	67.0	0
205-01	38.15	0	79.0	16
-02	44.88	0	86.75	28
-03	51.61	0	93.25	37
-04	60.59	0	107.5	58
-05	76.30	0	130.5	92
-06	67.32	0	106.0	56
-07	83.03	0	138.0	103
-08	89.76	0	147.0	116
-09	38.1	0.026	80.0	19
-10	"	0.035	82.0	22
-11	"	0.044	83.0	24
-12	"	0.05	86.0	28
-13	"	0.077	83.0	24
-14	"	0.10	86.0	28
-15	"	0.15	85.0	27
-16	"	0.20	85.0	27
-17	"	0.25	83.0	24
-18	44.9	0.026	89.0	33
-19	"	0.035	90.0	34
-20	"	0.044	87.0	30
-21	"	0.05	89.0	33
-22	"	0.077	91.0	36
-23	"	0.10	95.0	42
-24	"	0.15	94.0	40
-25	"	0.20	90.0	34
-26	"	0.25	85.0	27
-27	67.3	0.026	114.0	70
-28	"	0.035	118.0	76
-29	"	0.044	119.0	78
-30	"	0.05	120.0	79
-31	"	0.077	124.0	85
-32	89.8	0.035	152.0	127
-33	"	0.044	153.0	128
-34	"	0.050	154.0	130

IAV/ml
12/20/78

TABLE X

CALCULATED HOLDUPS IN CATALYST DENSE PHASE
FOR THREE-PHASE TESTS, RUN 201

Test No.	ϵ_{CB}	$\epsilon_l \gamma_B$	$\epsilon_g \gamma_B$	V_{CD} (mm/sec)
201-12	0.40	0.46	0.15	8.8
-13	0.40	0.49	0.11	4.0
-14	0.40	0.43	0.17	4.0
-15	0.42	0.40	0.18	5.6
-16	0.43	0.33	0.23	9.8
-17	0.43	0.32	0.25	13.7
-18	0.43	0.30	0.27	23.3
-19	0.43	0.28	0.32	29.8
-20	0.43	0.24	0.33	37.0
-21	0.43	0.47	0.10	3.0
-22	0.43	0.46	0.11	4.9
-23	0.40	0.49	0.11	7.6
-24	0.40	0.49	0.12	9.0
-25	0.38	0.44	0.18	12.4
-26	0.36	0.42	0.22	15.2
-27	0.34	0.42	0.23	25.1
-28	0.34	0.39	0.27	33.7
-29	0.34	0.38	0.28	43.5
-30	0.34	0.63	0.03	6.3
-31	0.36	0.56	0.08	5.9
-32	0.36	0.55	0.09	7.6
-33	0.35	0.55	0.10	8.7
-34	0.34	0.54	0.13	14.1
-35	0.33	0.49	0.19	15.4
-36	0.32	0.42	0.27	19.4
-37	0.29	0.43	0.28	29.6
-38	0.29	0.64	0.07	2.3
-39	0.29	0.63	0.09	3.1
-40	0.28	0.62	0.10	4.2
-41	0.28	0.60	0.12	4.7
-42	0.28	0.55	0.18	5.4
-43	0.34	0.35	0.31	--
-44	0.28	0.42	0.30	8.9

EMB/ml
10/6/78

TABLE XI

CALCULATED HOLDUPS IN CATALYST DENSE PHASE
FOR RUN 201

Test	ϵ_{c_B}	$\epsilon_{l\gamma_B}$	$\epsilon_{g\gamma_B}$	V_{CD} (mm/sec)
201-09	0.316	0.697	--	--
-10	0.276	0.712	--	--
-11	0.258	0.745	--	--
-45	0.336	0.333	0.331	31.32

EMB/ml
11/9/78

TABLE XII

CALCULATED HOLDUPS IN CATALYST DENSE PHASE
FOR RUN 203

Test	ϵ_{c_s}	$\epsilon_{l\gamma_s}$	$\epsilon_{g\gamma_s}$	V_{CD} (mm/sec)
203-01	0.50	0.57	0.0	--
-02	0.43	0.62	0.0	--
-03	0.34	0.69	0.0	--
-04	0.30	0.74	0.0	--
-05	0.44	0.40	0.16	7.8
-06	0.42	0.29	0.29	32.3
-07	0.37	0.51	0.12	7.1
-08	0.34	0.39	0.27	23.1
-09	0.31	0.57	0.13	4.8
-10	0.28	0.51	0.22	10.2
-11	0.27	0.62	0.11	4.0

EMB/ml
11/9/78

TABLE XIII

CALCULATED HOLDUPS IN CATALYST DENSE PHASE
FOR RUN 204

Test No.	ϵ_{c_B}	$\epsilon_{l_{\gamma_B}}$	$\epsilon_{g_{\gamma_B}}$	V_{CD} (mm/sec)
204-01	0.45	0.58	0.0	--
-02	0.38	0.63	0.0	--
-03	0.33	0.66	0.0	--
-04	0.31	0.67	0.0	--
-05	0.28	0.71	0.0	--
-06	0.25	0.73	0.0	--
-07	0.42	0.43	0.14	7.73
-08	0.45	0.44	0.12	2.52
-09	0.45	0.42	0.13	4.15
-10	0.44	0.40	0.16	4.58
-11	0.37	0.45	0.17	18.90
-12	0.38	0.38	0.24	24.90
-14	0.34	0.53	0.13	4.40
-15	0.34	0.54	0.12	6.90
-16	0.31	0.56	0.13	7.86
-17	0.29	0.47	0.24	13.90
-18	0.27	0.66	0.07	3.80
-19	0.26	0.64	0.09	6.45
-20	0.26	0.62	0.12	5.75
-21	0.26	0.61	0.14	6.90
-22	0.24	0.69	0.08	3.98
-23	0.23	0.67	0.10	4.68
-24	0.24	0.65	0.11	7.5
-25	0.39	0.40	0.20	12.78
-26	0.43	0.46	0.11	3.42
-27	0.34	0.44	0.22	13.13
-28	0.29	0.63	0.08	4.50

EMB/ml
11/9/78

TABLE XIV

CALCULATED HOLDUPS IN CATALYST DENSE PHASE FOR RUN 205

Run No.	ϵ_{C_B}	$\epsilon_{l_{V_B}}$	$\epsilon_{g_{V_B}}$	V_{CD}
205-01	0.42	0.56	--	--
-02	0.38	0.59	--	--
-03	0.35	0.60	--	--
-04	0.31	0.64	--	--
-05	0.25	0.66	--	--
-06	0.28	0.64	--	--
-07	0.24	0.69	--	--
-08	0.22	0.71	--	--
-09	0.39	0.483	0.071	5.52
-10	0.39	0.484	0.070	7.85
-11	0.38	0.475	0.090	9.68
-12	0.38	0.448	0.120	9.18
-13	0.40	0.388	0.167	12.3
-14	0.35	0.429	0.171	18.7
-15	0.38	0.373	0.204	27.1
-16	0.38	0.373	0.204	38.9
-17	0.40	0.353	0.206	50.4
-18	0.37	0.521	0.0485	7.42
-19	0.36	0.497	0.085	7.5
-20	0.38	0.455	0.112	7.68
-21	0.36	0.481	0.103	10.0
-22	0.37	0.430	0.150	12.7
-23	0.34	0.444	0.164	18.1
-24	0.34	0.415	0.197	27.5
-25	0.37	0.410	0.172	41.6
-26	0.39	0.351	0.218	47.9
-27	0.29	0.556	0.089	4.72
-28	0.28	0.610	0.039	11.5
-29	0.28	0.583	0.069	12.9
-30	0.28	0.574	0.079	13.0
-31	0.27	0.525	0.144	14.2
-32	0.22	0.672	0.030	12.44
-33	0.22	0.661	0.042	14.1
-34	0.21	0.641	0.075	12.6

IAV/ml
12/20/78

TABLE XV

RICHARDSON-ZAKI INDEX
FOR RUNS 203, 204, AND 205

Run	n
201	2.9
203	3.2
204	3.4
205	3.5

EMB/ml
11/9/78

TABLE XVI

DISTRIBUTION OF COAL CHAR
IN REACTOR RUNS 204 AND 205

Reactor Position	Run 204, Vol%	Run 205, Vol%
Base	4.94	9.65
62"	5.02	9.78
124"	4.45	10.95
186"	7.96	11.16
Average	5.6	10.4
Nominal Concentration	5.0	10.0

IAV/ml
12/20/78

TABLE XVII

TEST CONDITIONS FOR A-41 RADIOTRACER TESTS

Test No.	U_l Feed (Ft/Sec)	U_l Recycle (Ft/Sec)	U_g (Ft/Sec)
1	0.015	0.085	0.035
2	0.015	0.085	0.035
3	0.015	0.085	0.035
4	0.10	0.0	0.2
5	0.10	0.0	0.15
6	0.10	0.0	0.10
7	0.028	0.172	0.10
8	0.028	0.172	0.10
9	0.028	0.142	0.05
10	0.033	0.167	0.05
11	0.033	0.167	0.10
12	0.033	0.167	0.13
13	0.033	0.167	0.13
14	0.029	0.189	0.05
15	0.029	0.189	0.05
16	0.029	0.189	0.25

EMB/ml
10/6/78

TABLE XVIII

RADIOACTIVE GAS TRACER TEST DATA

Test No.	Detector No.	m(1)	m(2)
3	2	28.7	257
	3	64.1	1097
	4	112.6	3218
	5	--	--
4	2	16.3	127
	3	44.8	587
	4	86.7	2019
	5	119.7	6552
5	2	12.1	40
	3	27.3	83
	4	62.6	868
	5	84.1	1702
6	2	14.4	71
	3	32.6	205
	4	61.5	685
	5	96.0	2132
8	2	13.2	25
	3	27.9	64
	4	47.9	174
	5	69.3	506
9	2	16.0	84
	3	35.2	182
	4	60.7	412
	5	88.0	1116
10	2	13.3	41
	3	30.1	100
	4	50.4	230
	5	73.8	649
11	2	10.6	14
	3	24.9	71
	4	40.3	103
	5	57.3	327
13	2	12.7	36
	3	27.9	144
	4	40.3	120
	5	55.5	267
15	2	16.5	97
	3	28.0	68
	4	47.4	176
	5	63.7	324

m(1) = first moment, average residence time.
m(2) = second moment, variance.

EMB/ml

TABLE XIX

CALCULATED GAS HOLDUPS FROM GAS RADIOACTIVE TRACER TESTS

Test No.	Dense Phase ϵ_g	Dilute Phase ϵ_g
3	0.17 (0.08)	0.315 (0.06)
4	0.55 (0.28)	---
5	0.30 (0.27)	0.60 (0.30)
6	0.24 (0.19)	0.54 (0.20)
8	0.22	0.37
9	0.13 (0.12)	0.24 (0.09)
10	0.11	0.19
11	0.18	0.28
13	0.28	0.30
15	0.14	0.18

( ) values calculated from gamma-ray scans.

EMB/ml
12/20/78

Figure 1

% BED EXPANSION VS. U_g; RUN 201, KEROSENE/0% FINES

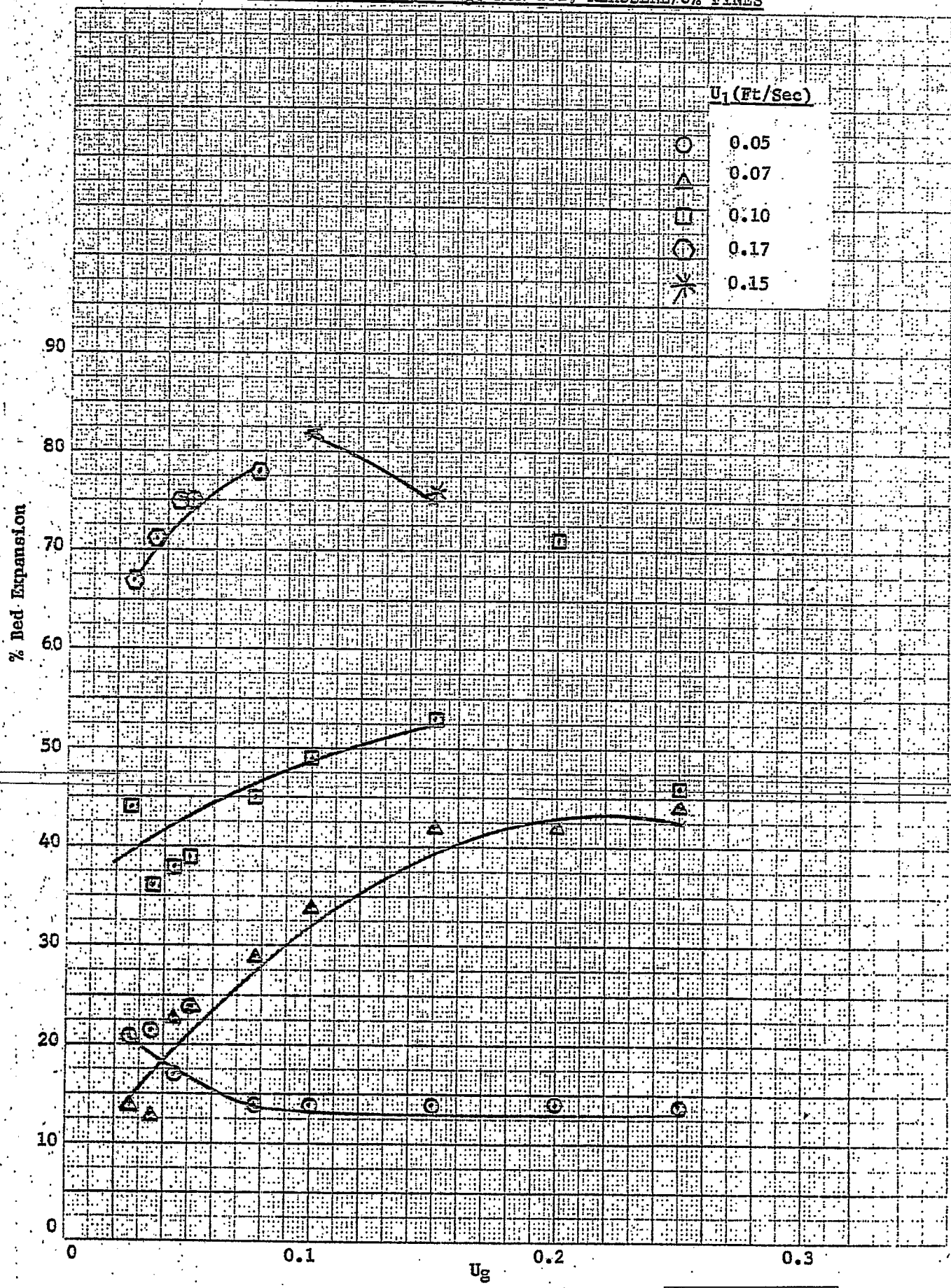

Figure 2

% BED EXPANSION VS. U_g; RUN 203, KEROSENE/1% FINES

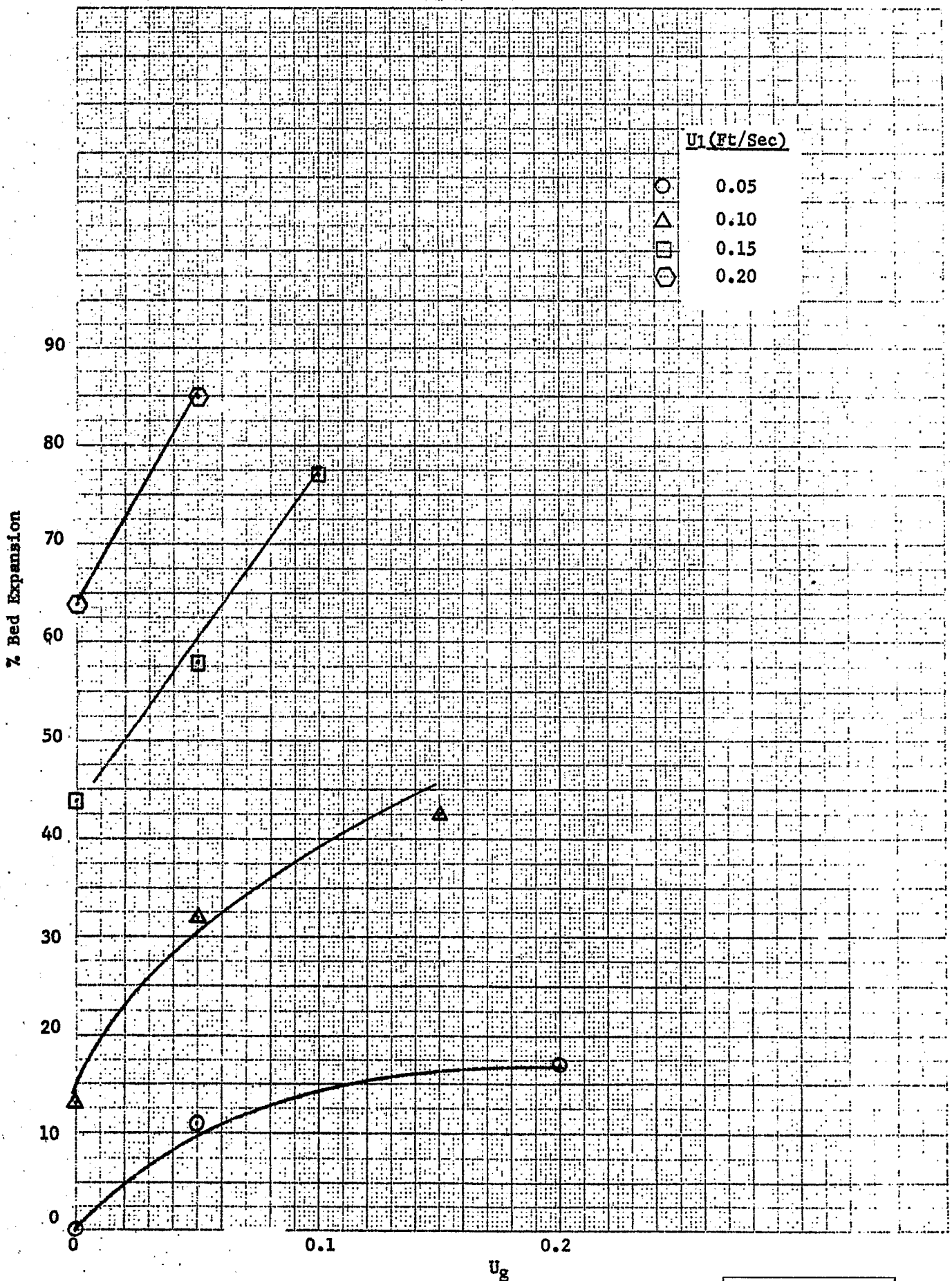

Figure 3

% BED EXPANSION VS. U_g; RUN 204, KEROSENE/5% FINES

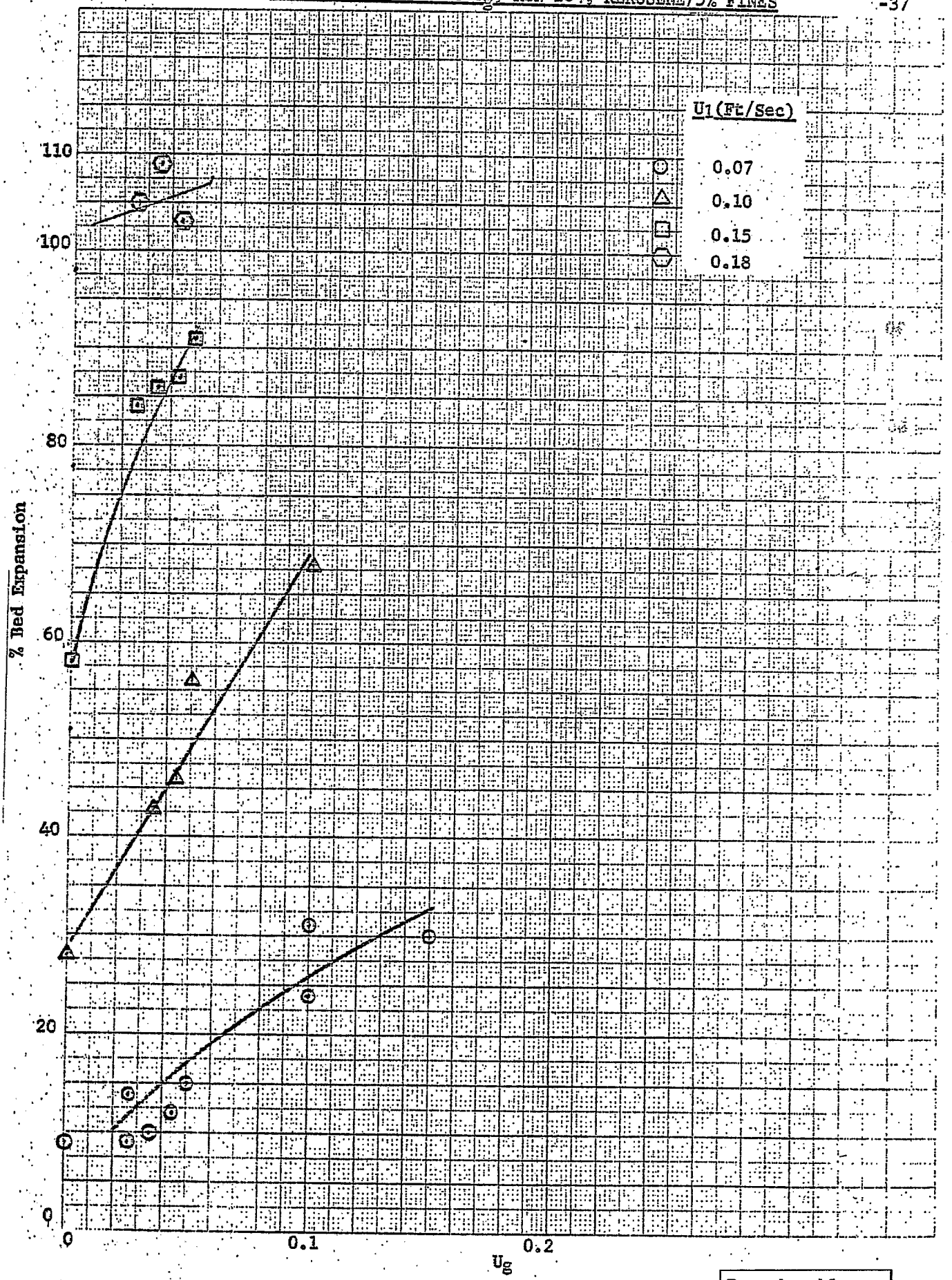

Figure 4

% BED EXPANSION VS. U_g; RUN 205, KEROSENE/10% FINES

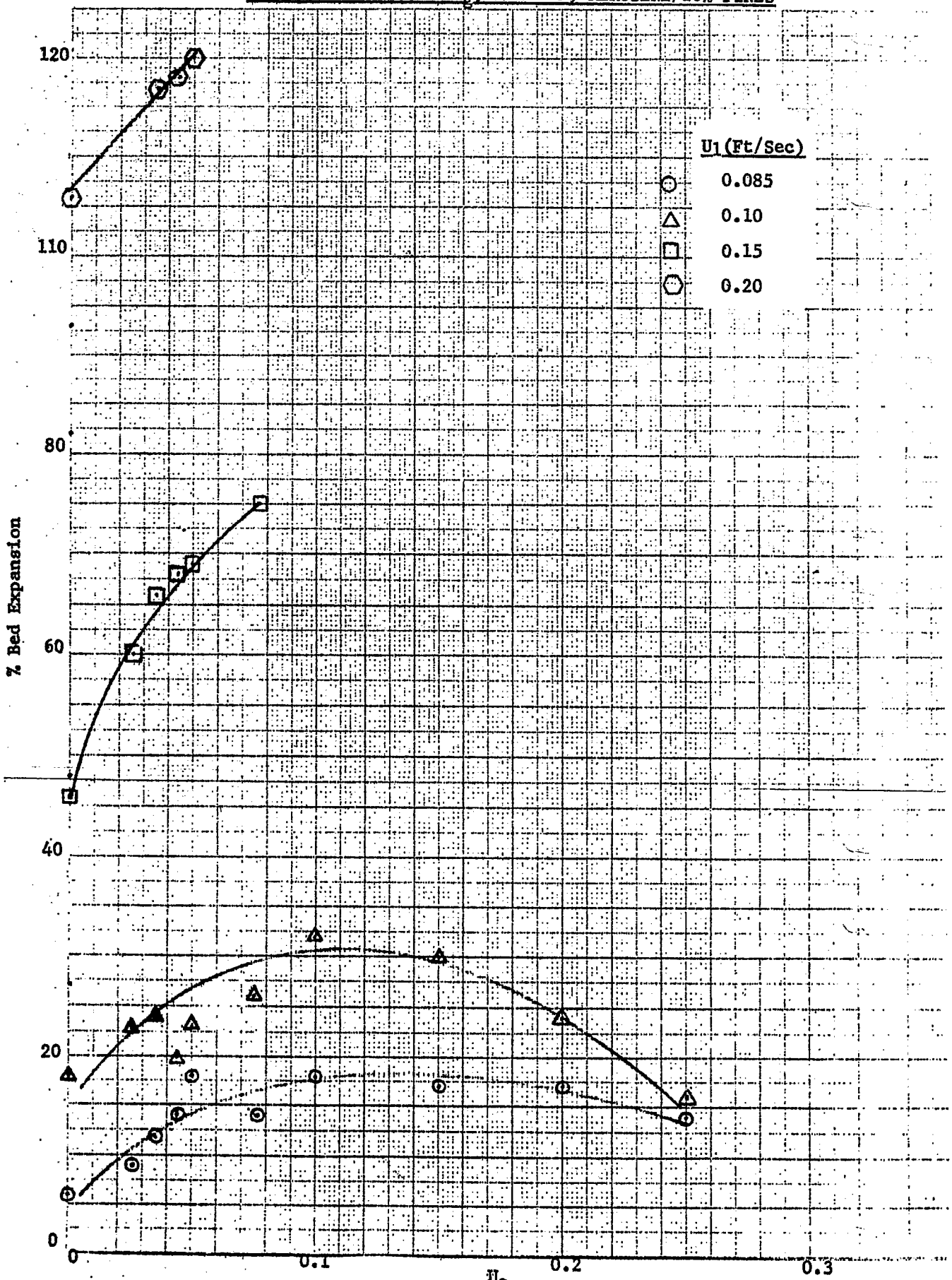

Figure 5

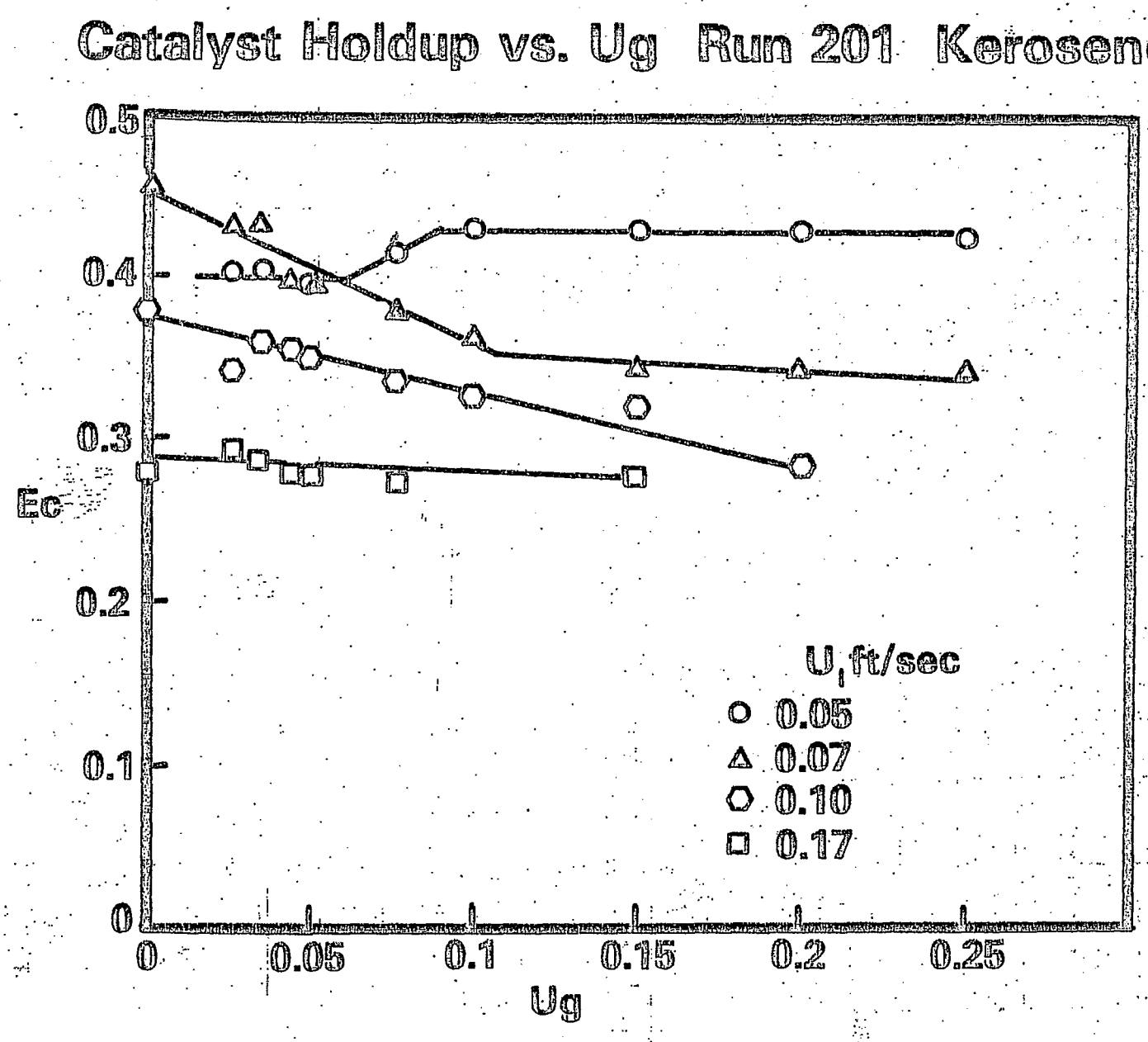
Catalyst Holdup vs. Ug Run 201 Kerosene
0.5
0.4
0.3
0.2
0.1
0
Ec
0
0.05
0.1
0.15
0.2
0.25
Ug
U, ft/sec
0.05
0.07
0.10
0.17

Figure 6

Catalyst Holdup vs. Ug, Run 204, Kerosene + 5 vol% Coal Char

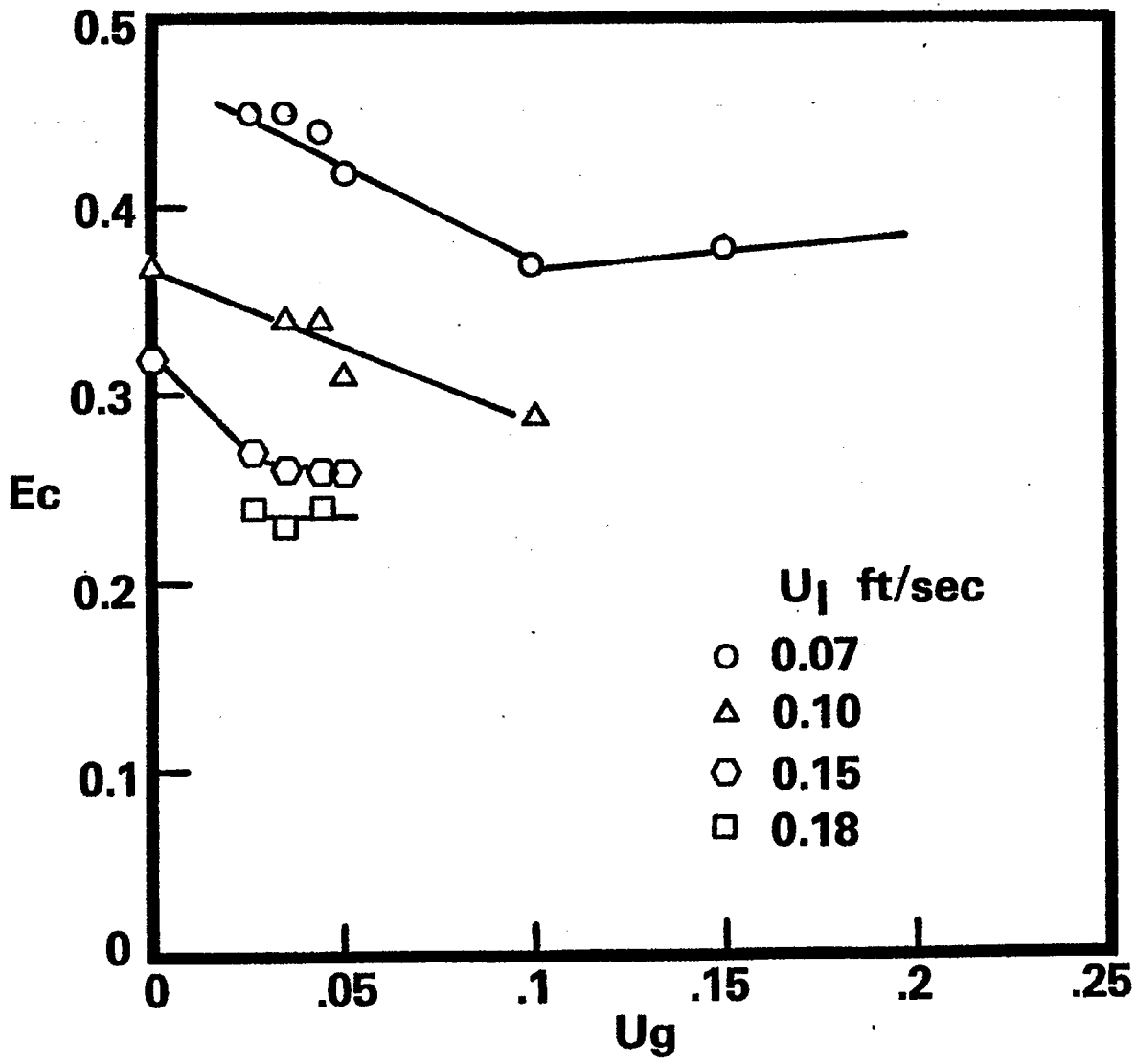

Figure 7

Catalyst Holdup vs. Ug, run 205, Kerosene + 10 vol% Coal Char

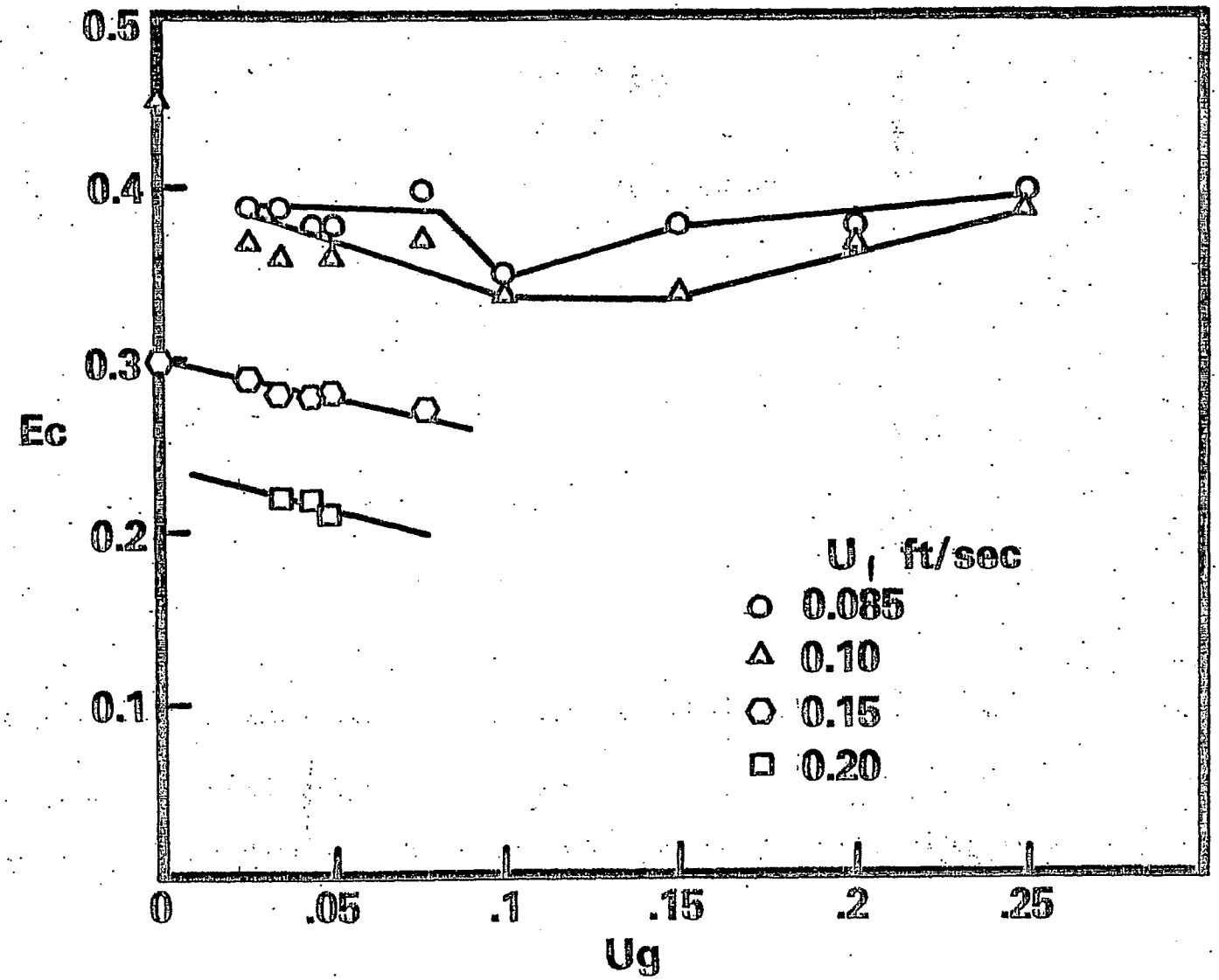

Figure 8

BED VOIDAGE VS. U_1/U_t, RUN 201

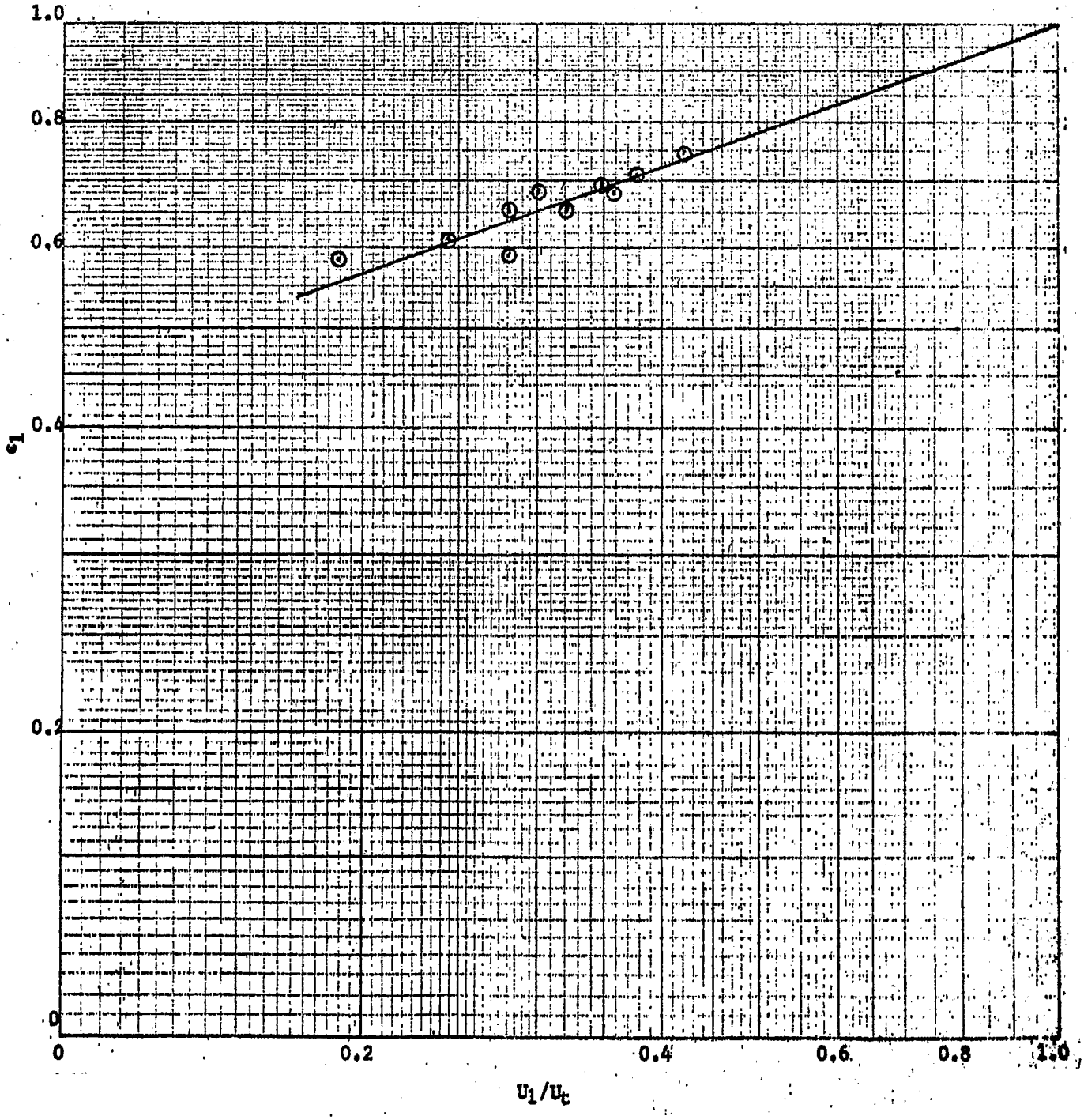

Figure 9

BED VOIDAGE VS. SUPERFICIAL LIQUID VELOCITY, RUN 203

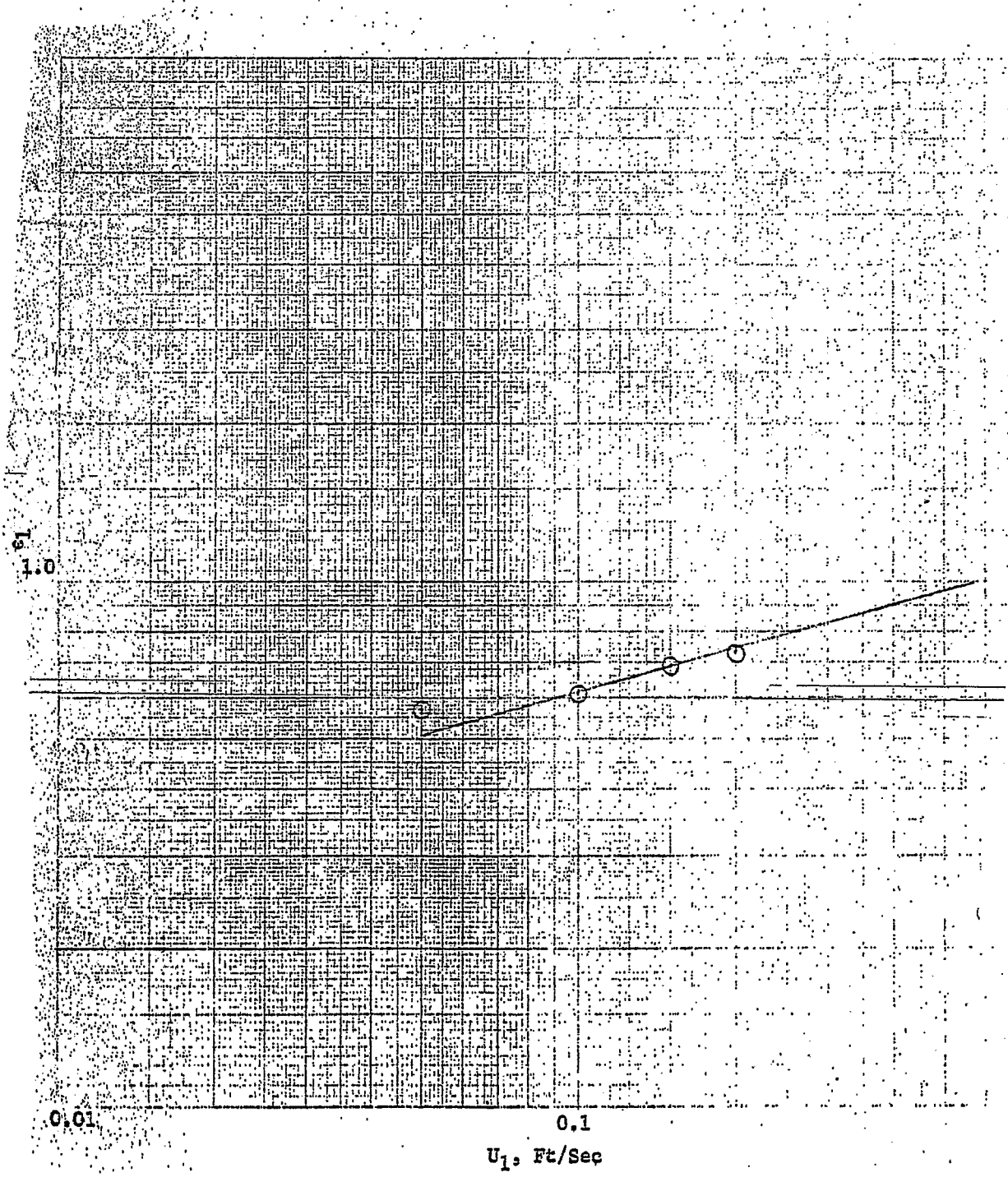

☆U.S. GOVERNMENT PRINTING OFFICE: 1979 -640 - 014 4623 REGION NO. 4

Figure 10

BED VOIDAGE VS. SUPERFICIAL LIQUID VELOCITY, RUN 204

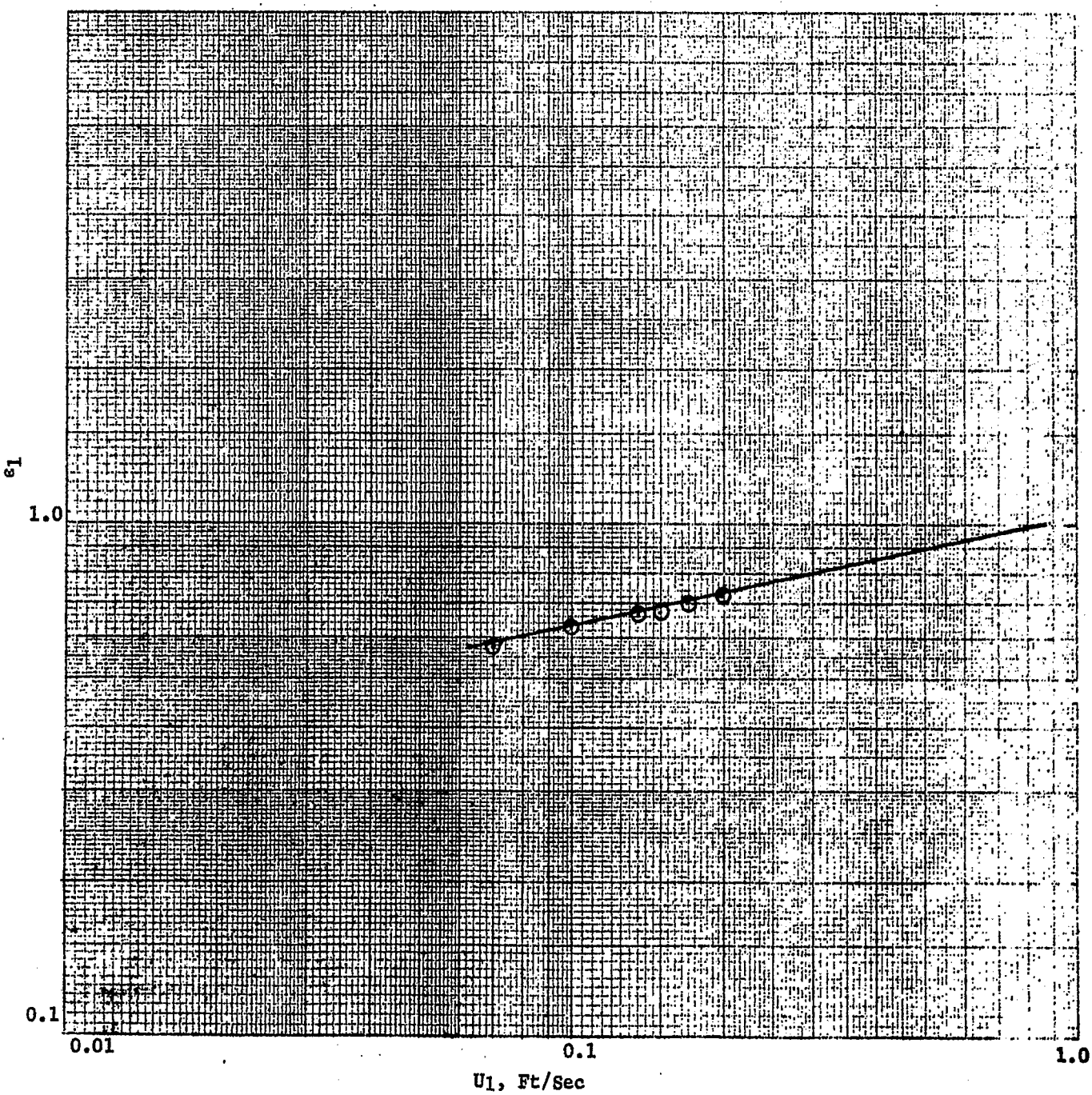

Figure 11

BED VOIDAGE VS. SUPERFICIAL LIQUID VELOCITY, RUN 205

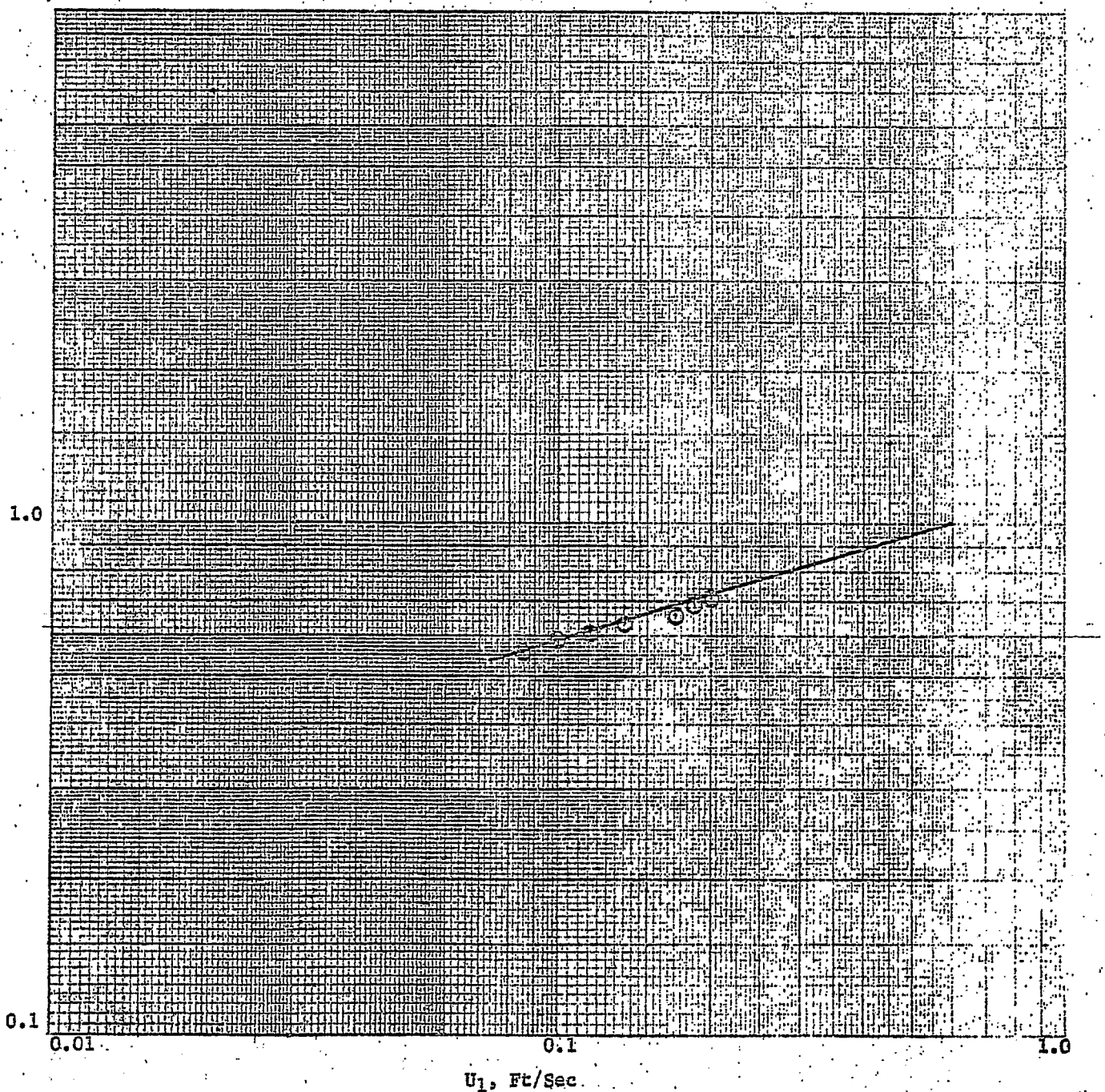

Figure 12

BED VOIDAGE VS. U_1/U_t, Run 203

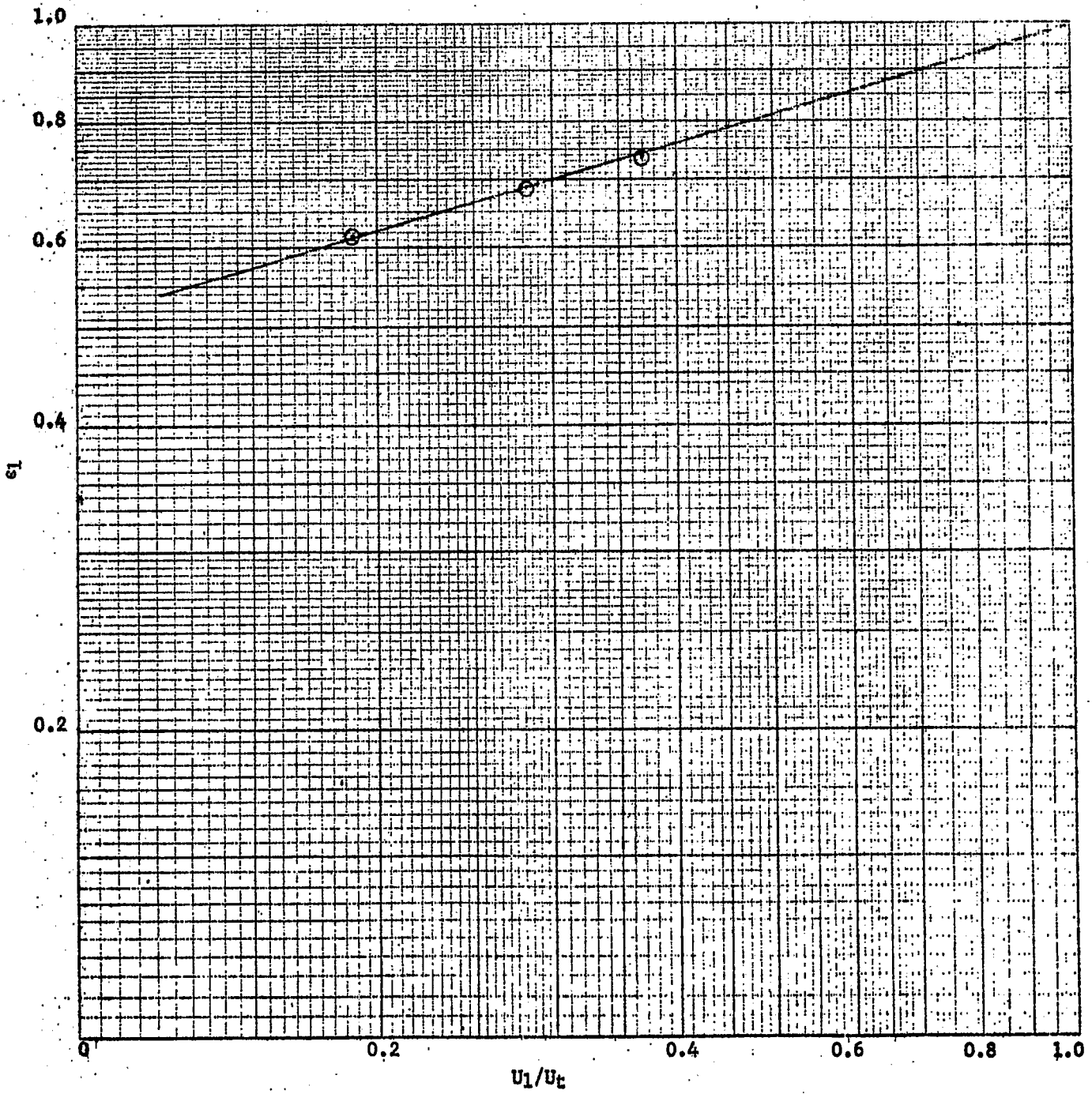

Figure 13

BED VOIDAGE VS. U_1/U_t, RUN 204

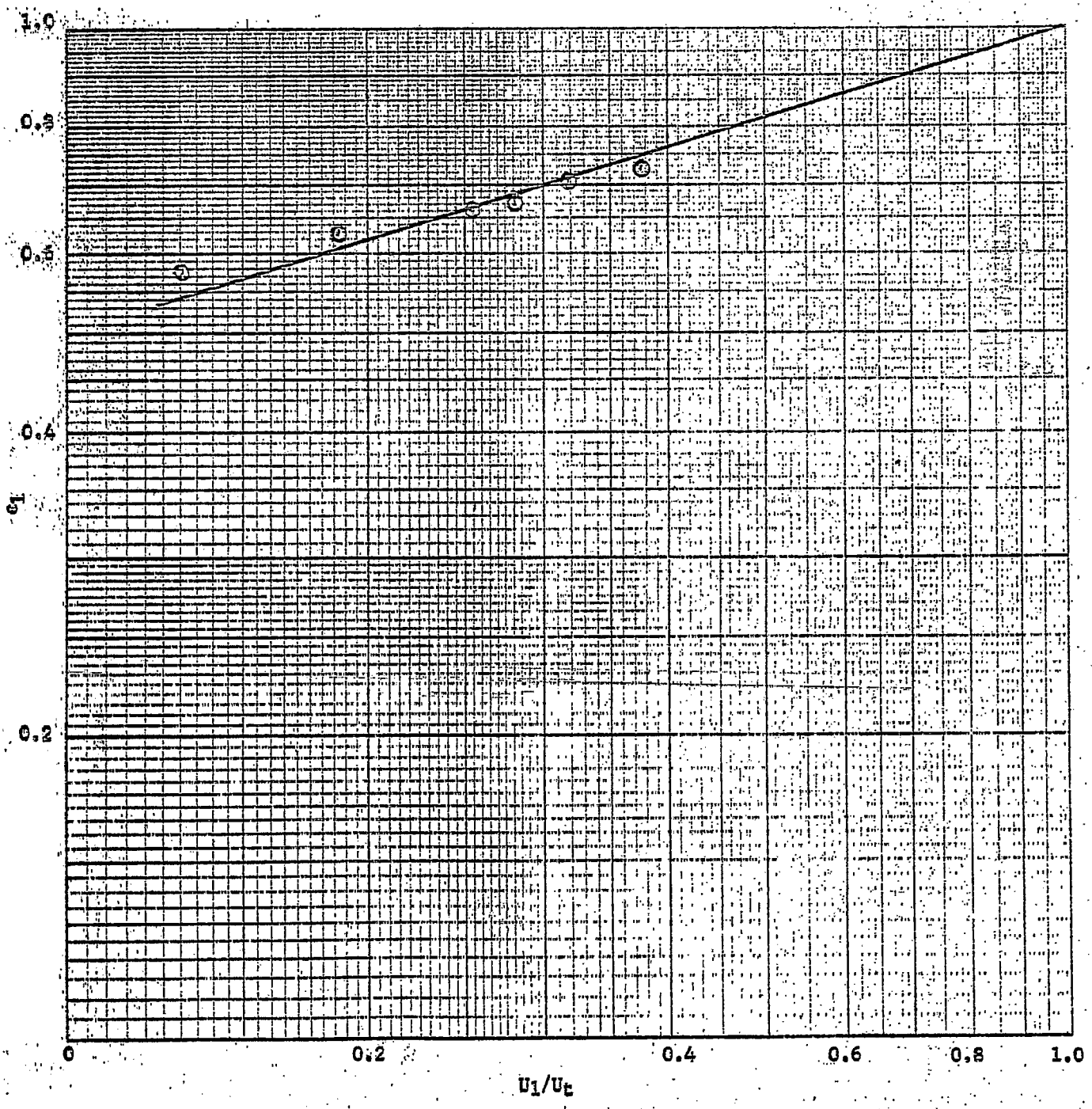

Figure 14

BED VOIDAGE VS. U_1/U_t, RUN 205

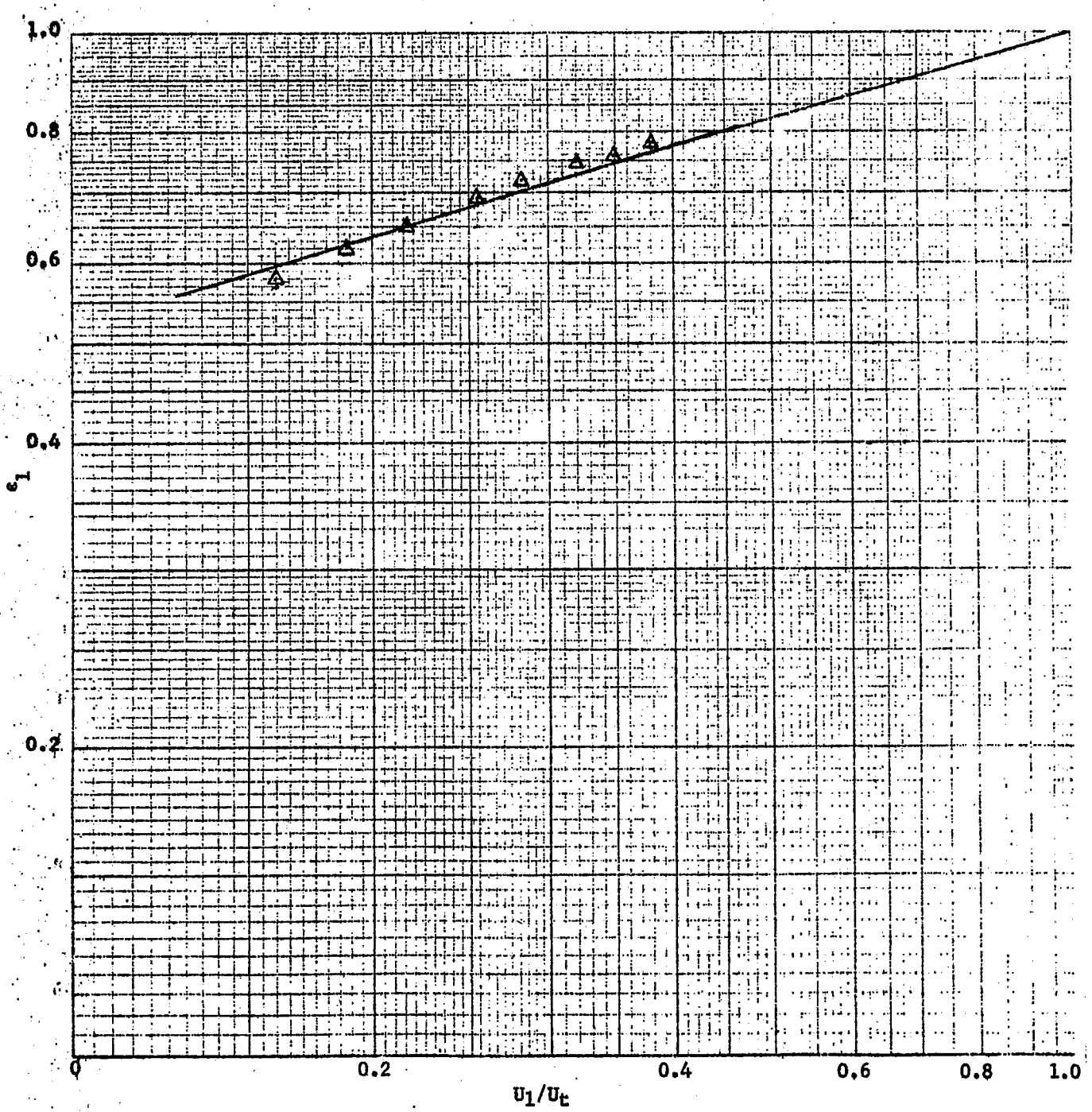

Figure 15

DRIFT FLUX VS. GAS HOLDUP, RUN 201

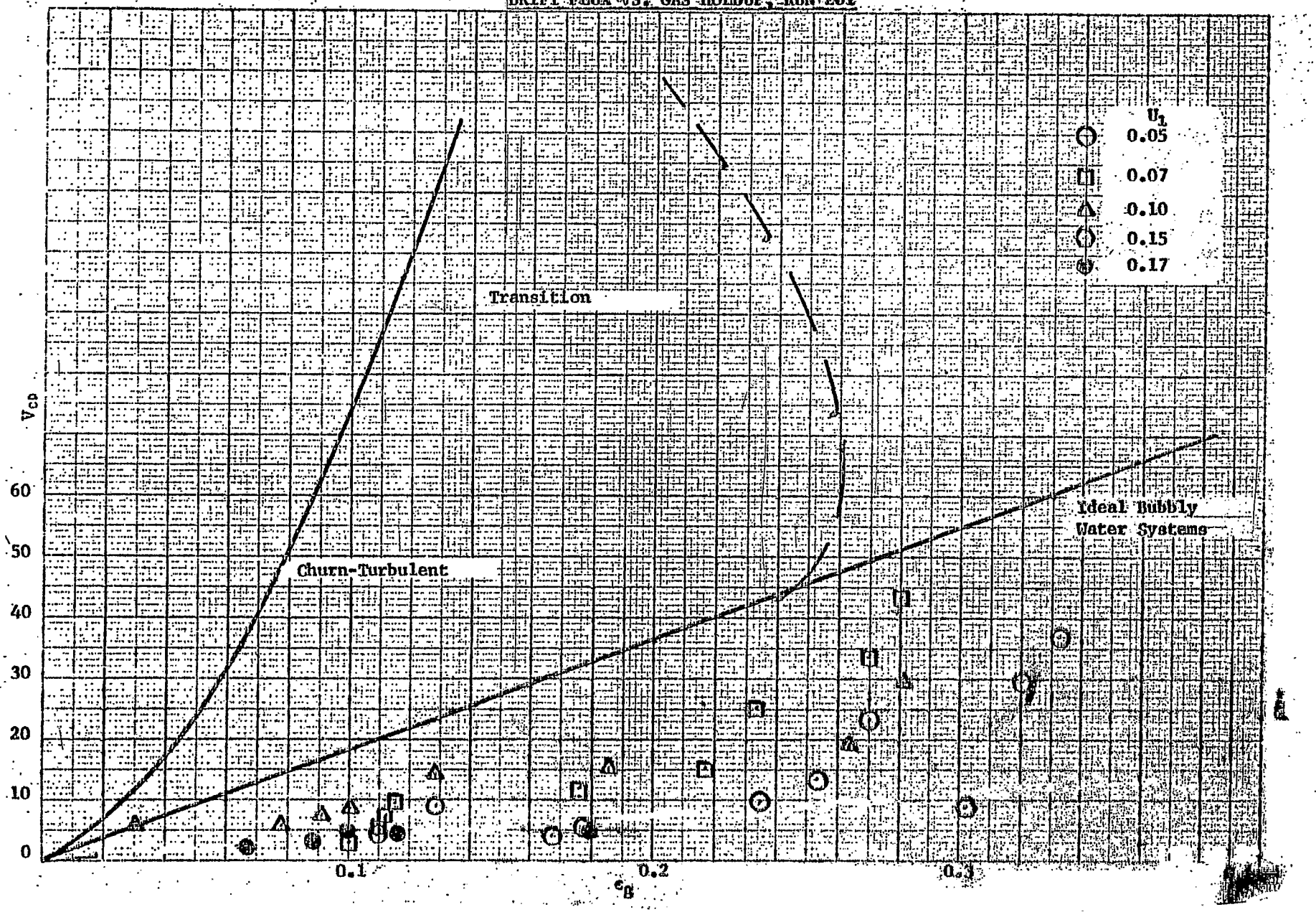

Figure 16

DRIFT FLUX VS. GAS HOLDUP, RUNS 203 AND 204

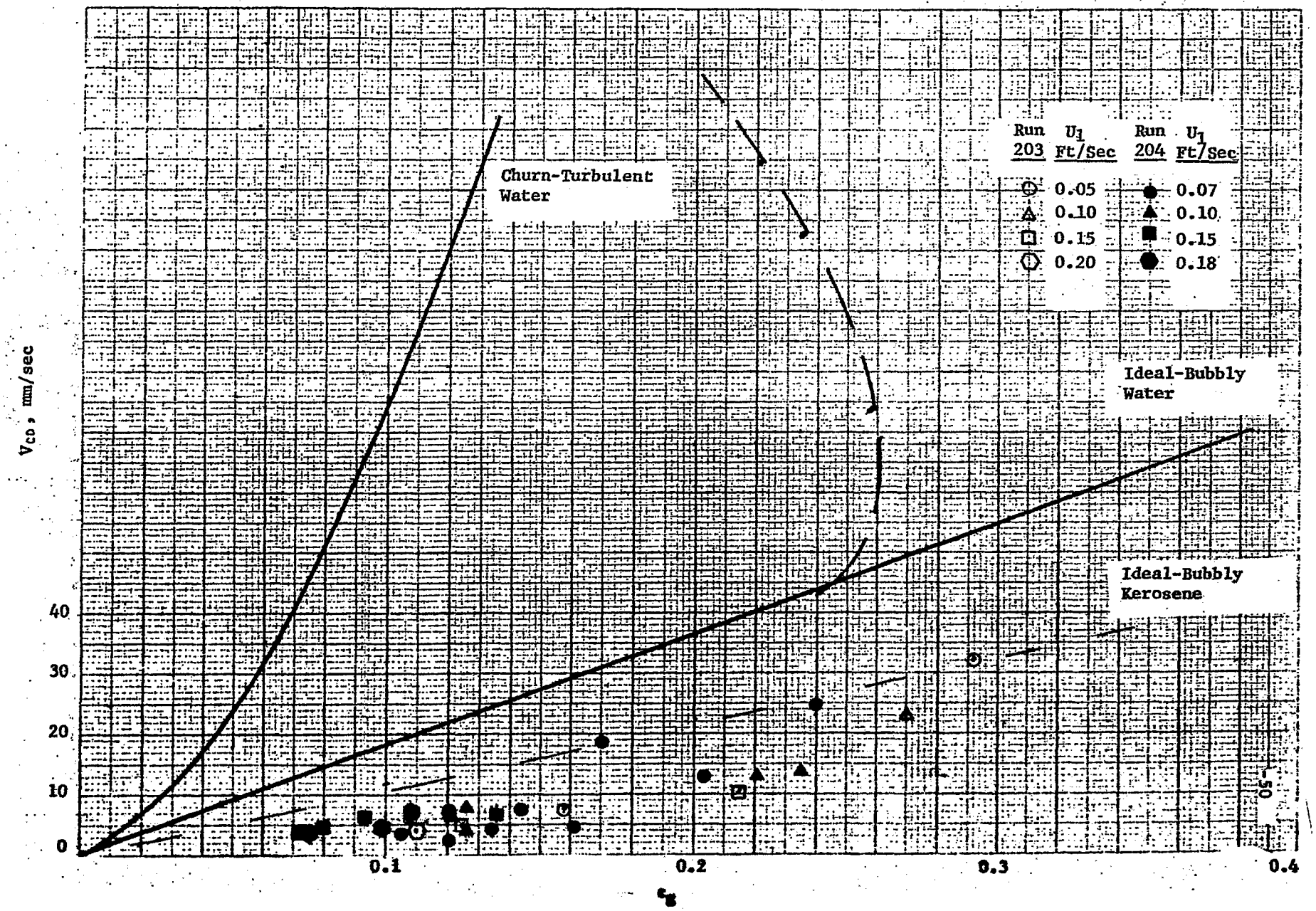

Figure 17

Drift Flux us. Gas Holdup, RUN 205

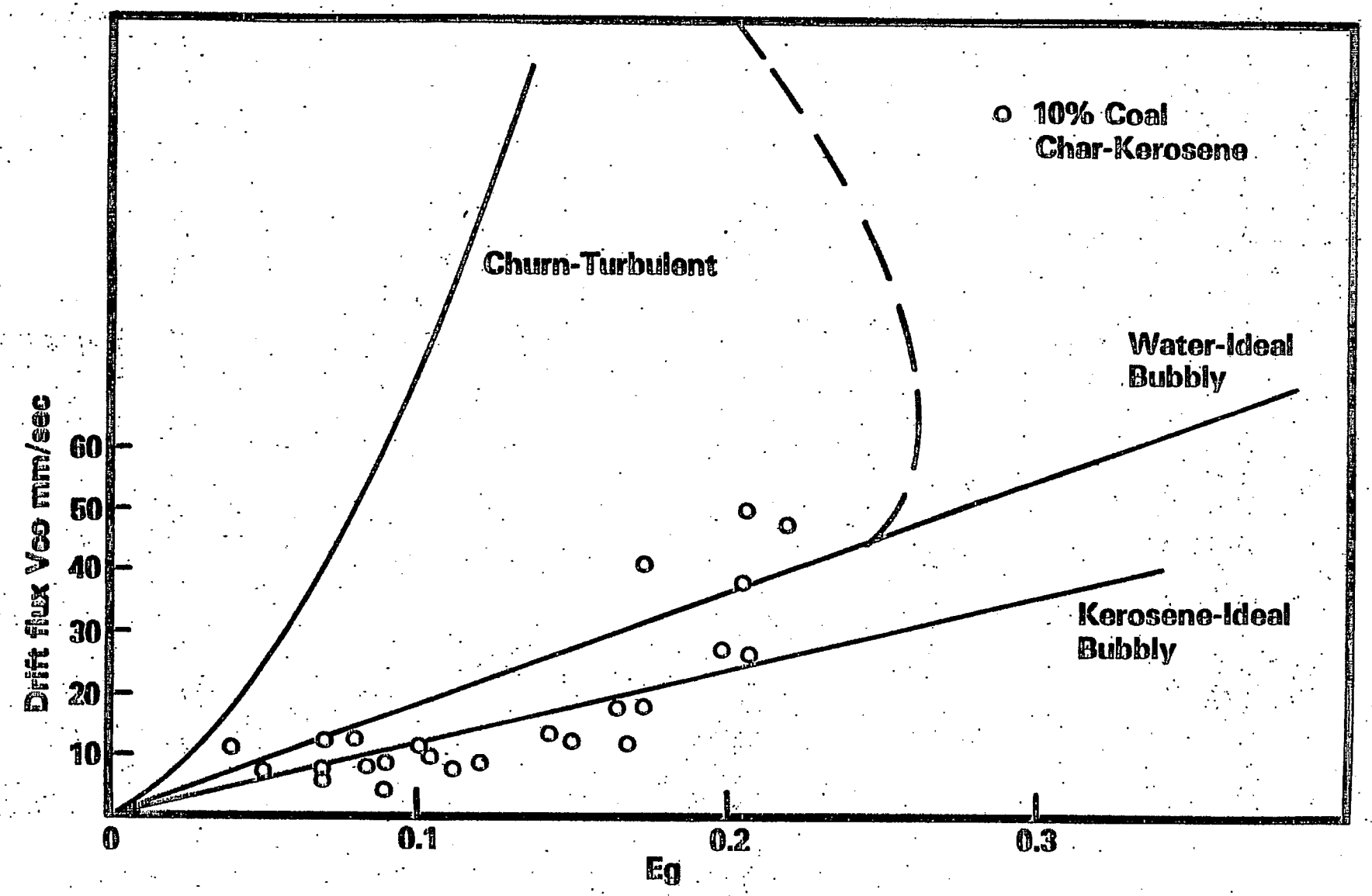

Figure 18

RADIOTRACER DETECTOR LOCATION:
H-COAL FLUID DYNAMICS FLOW SHEET

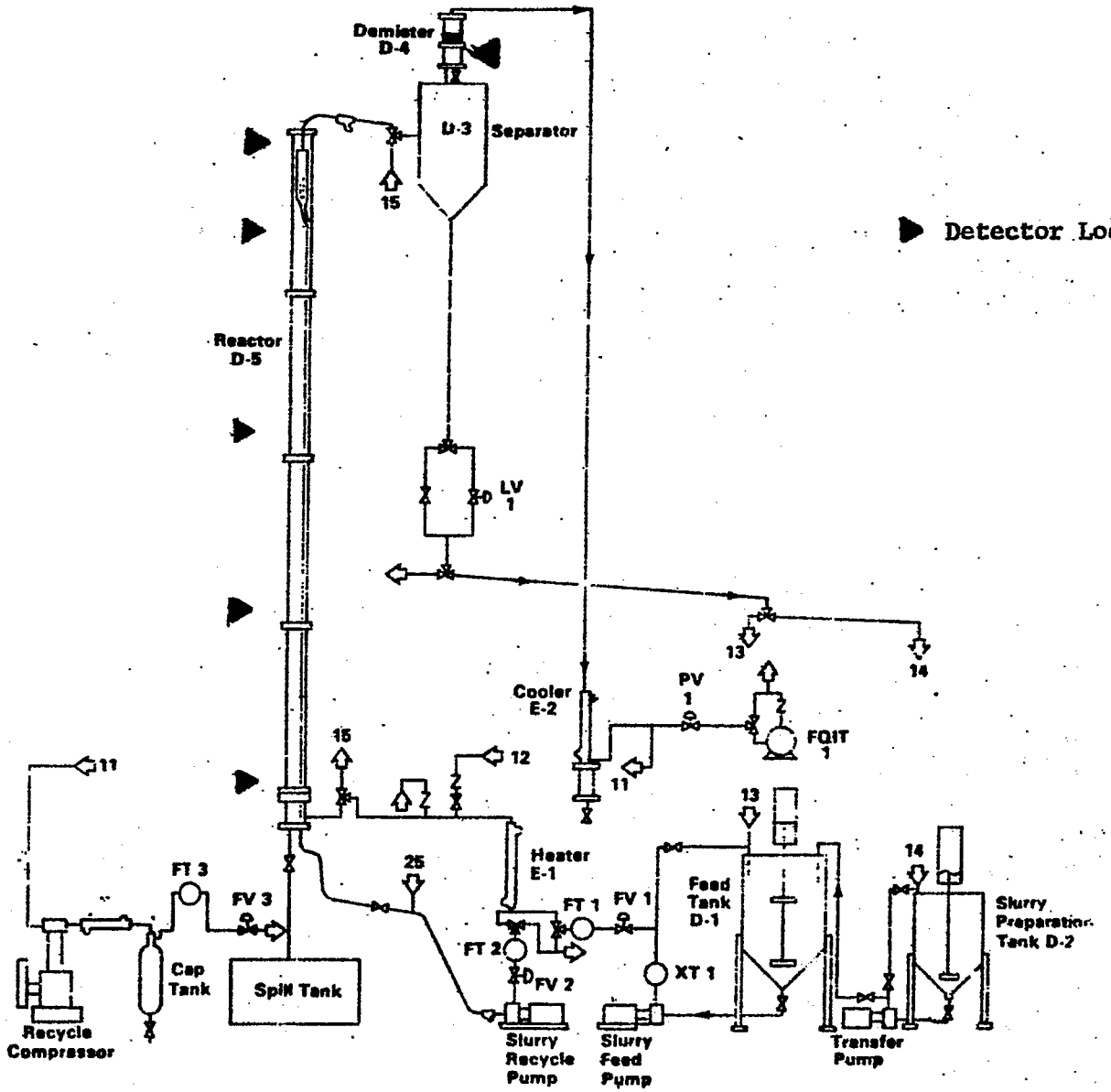

▶ Detector Location

Figure 19

RECORDER TRACER INJECTION OUTPUT, TEST 9

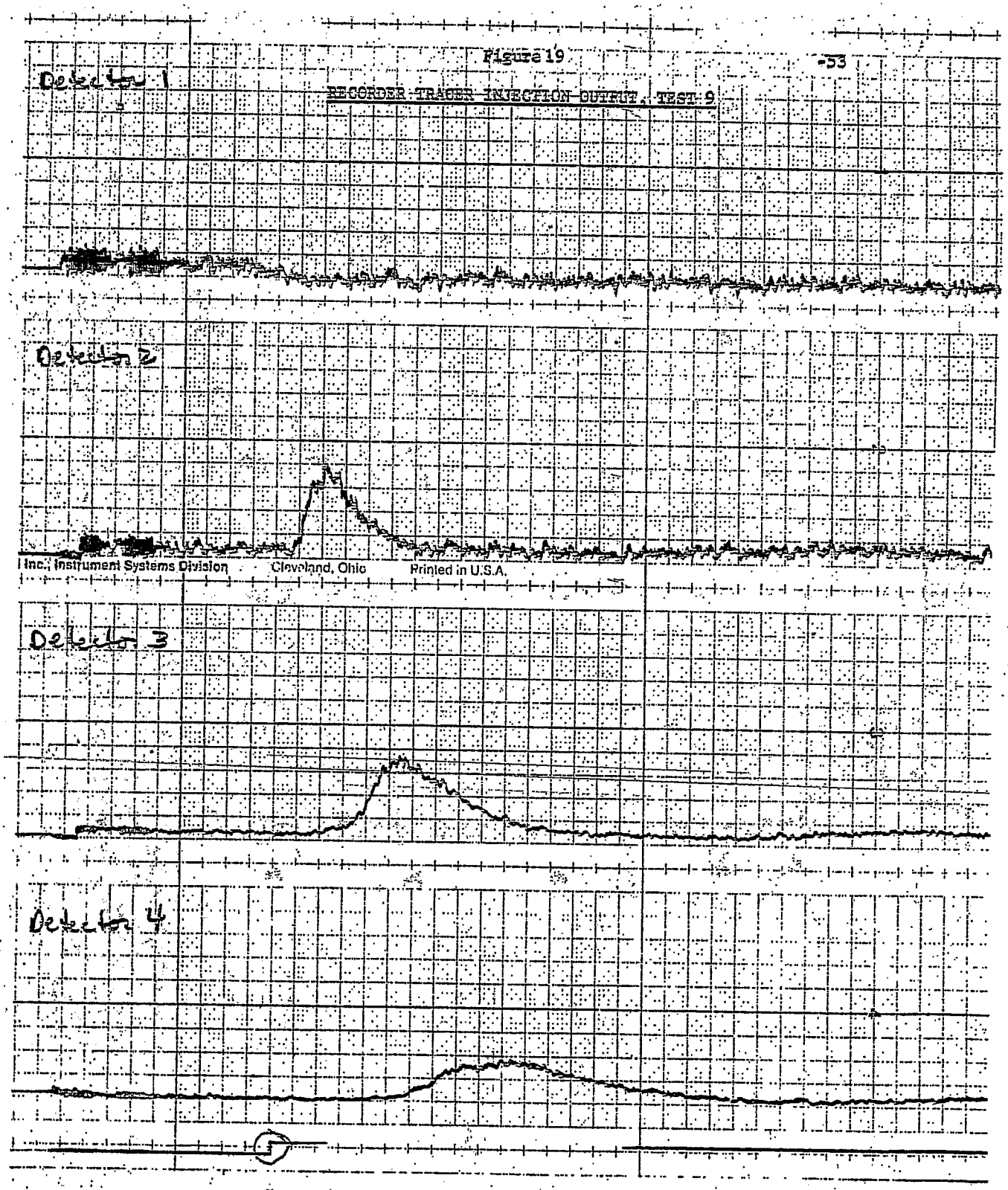

Figure 19
(Continued)

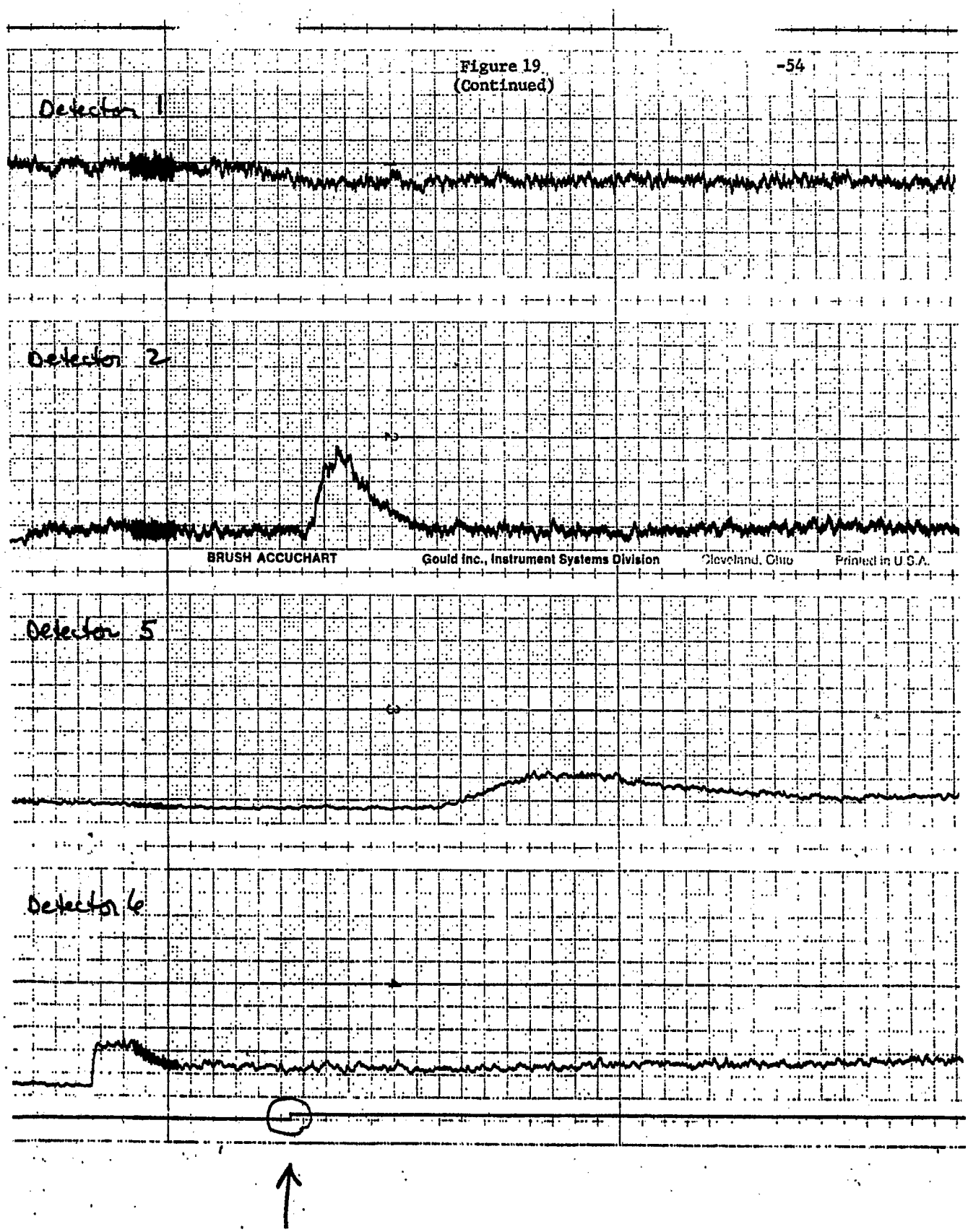

Figure 20

INTERNAL AGE AND INTENSITY FUNCTION VS. TIME: TEST 4

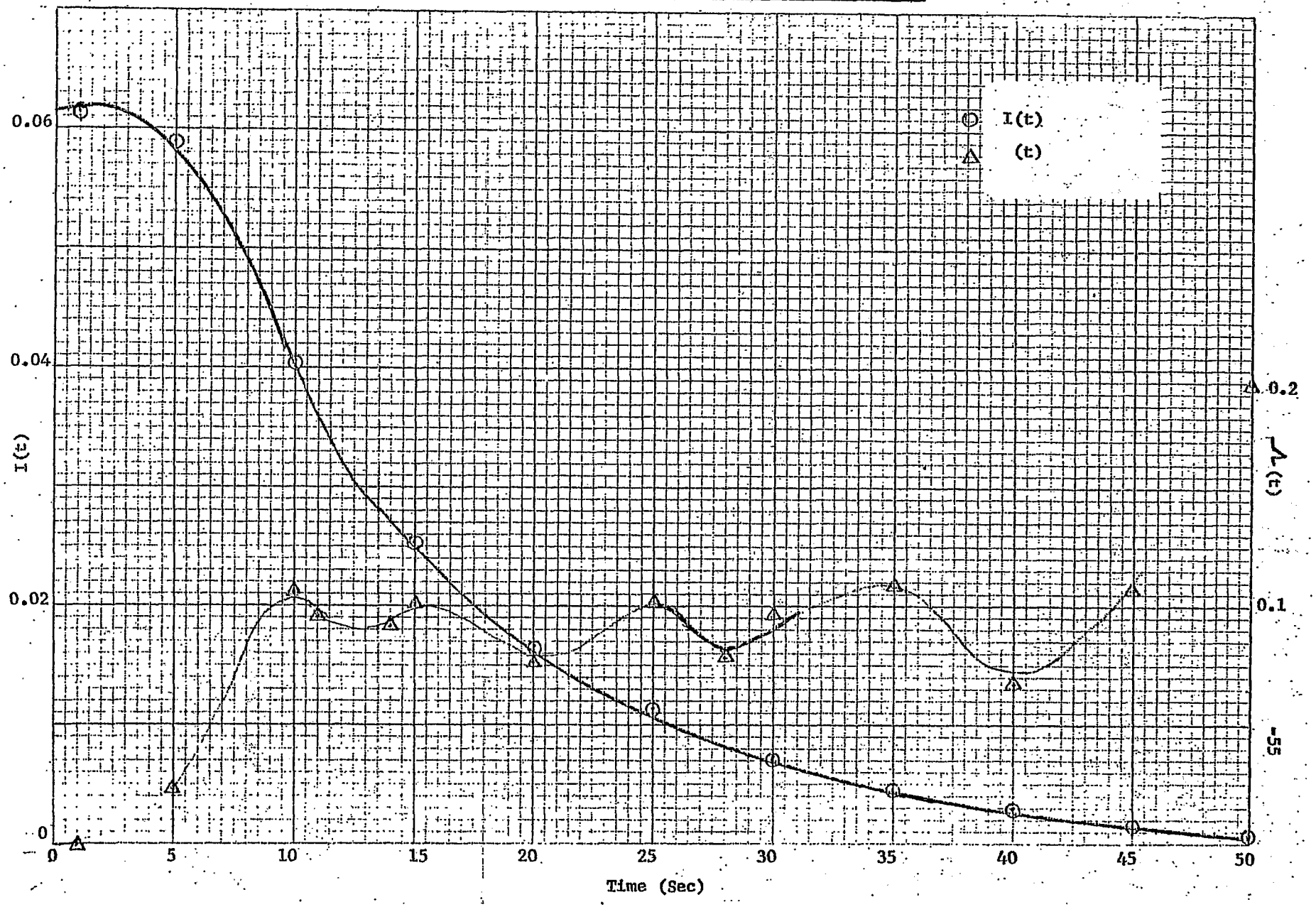

Figure 21

INTERNAL AGE AND INTENSITY FUNCTION VS. TIME; TEST 6

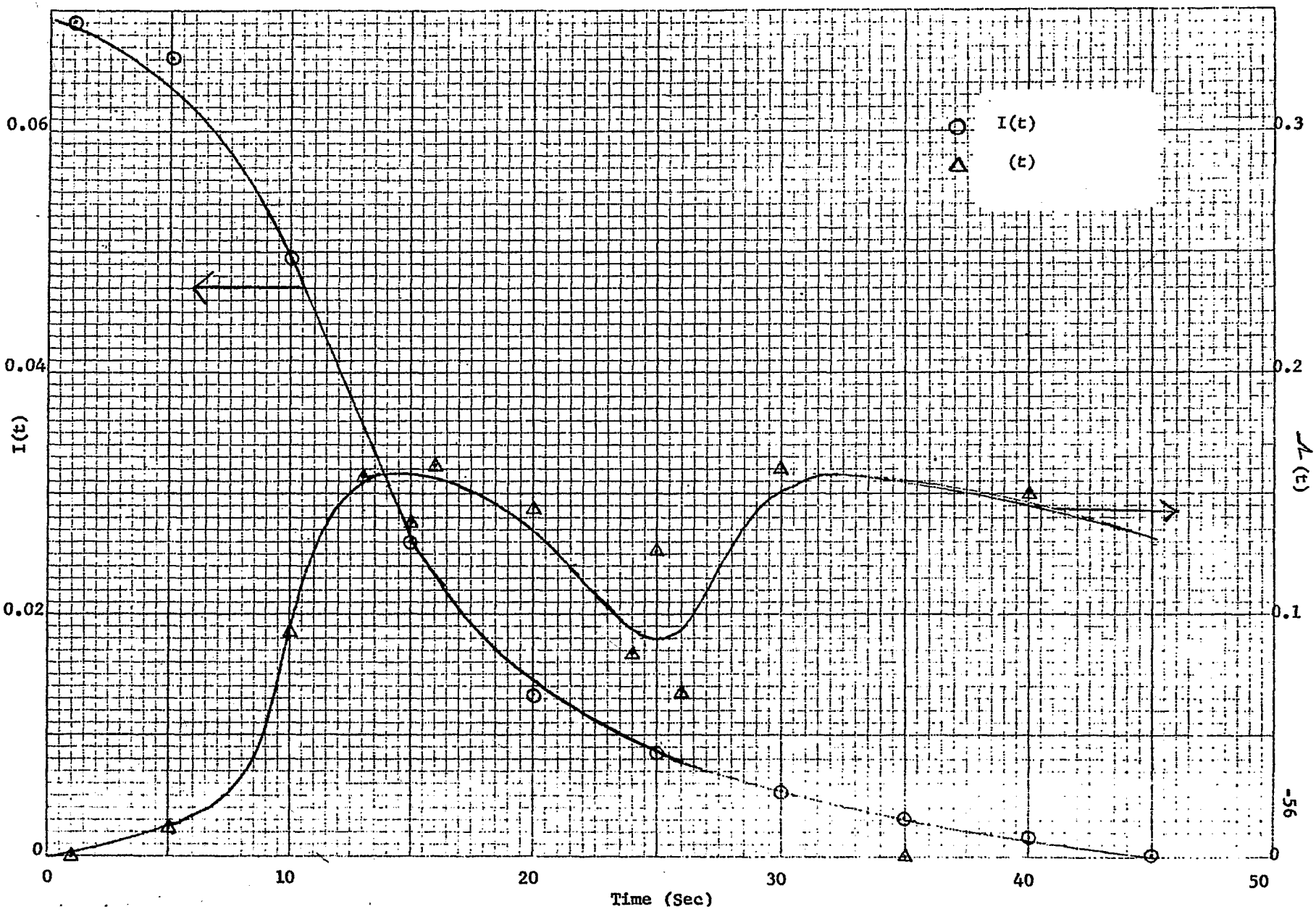

Figure 22

INTERNAL AGE AND INTENSITY FUNCTION VS. TIME; TEST 8

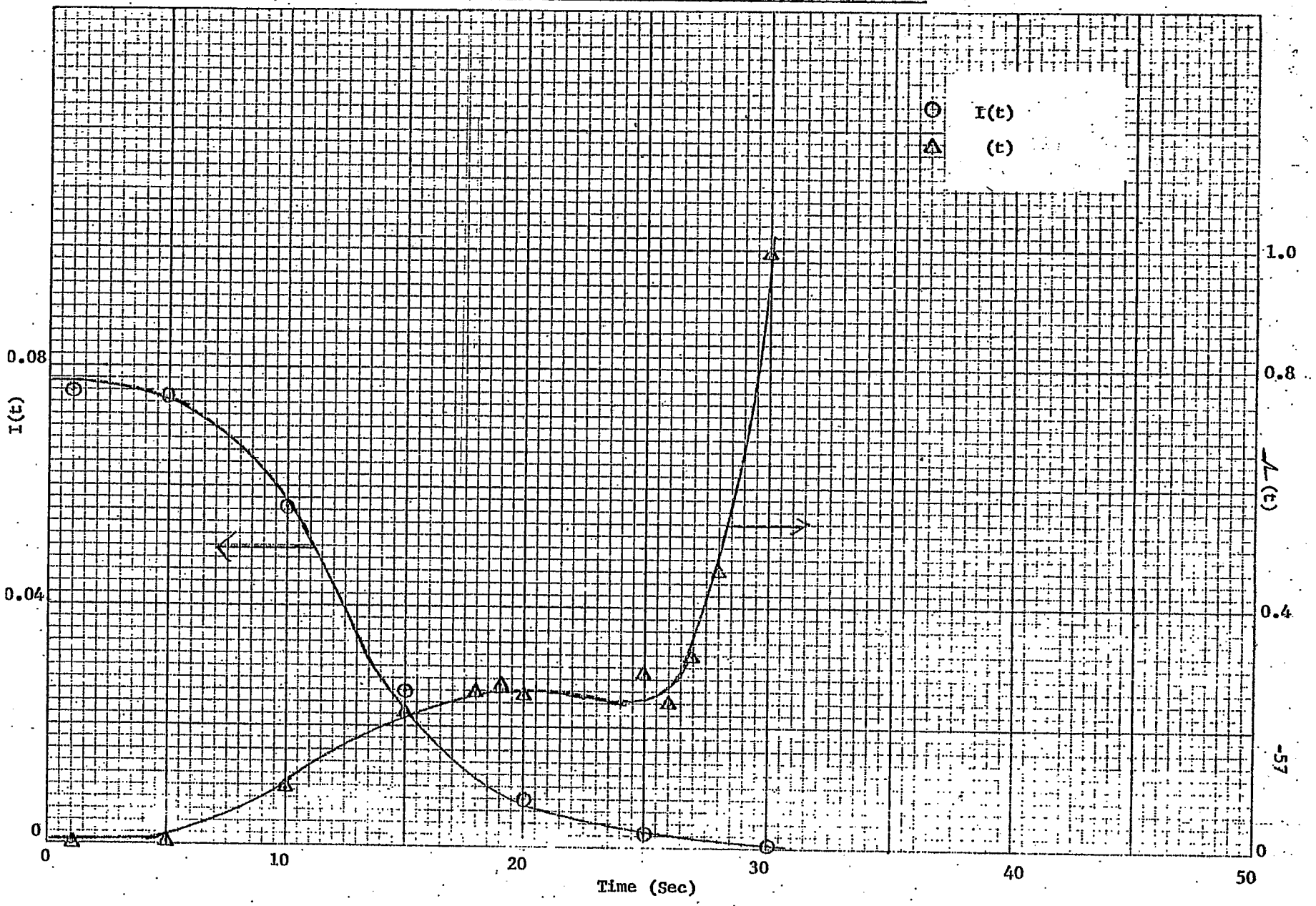

Figure 23

INTERNAL AGE AND INTENSITY FUNCTION VS. TIME; TEST 10

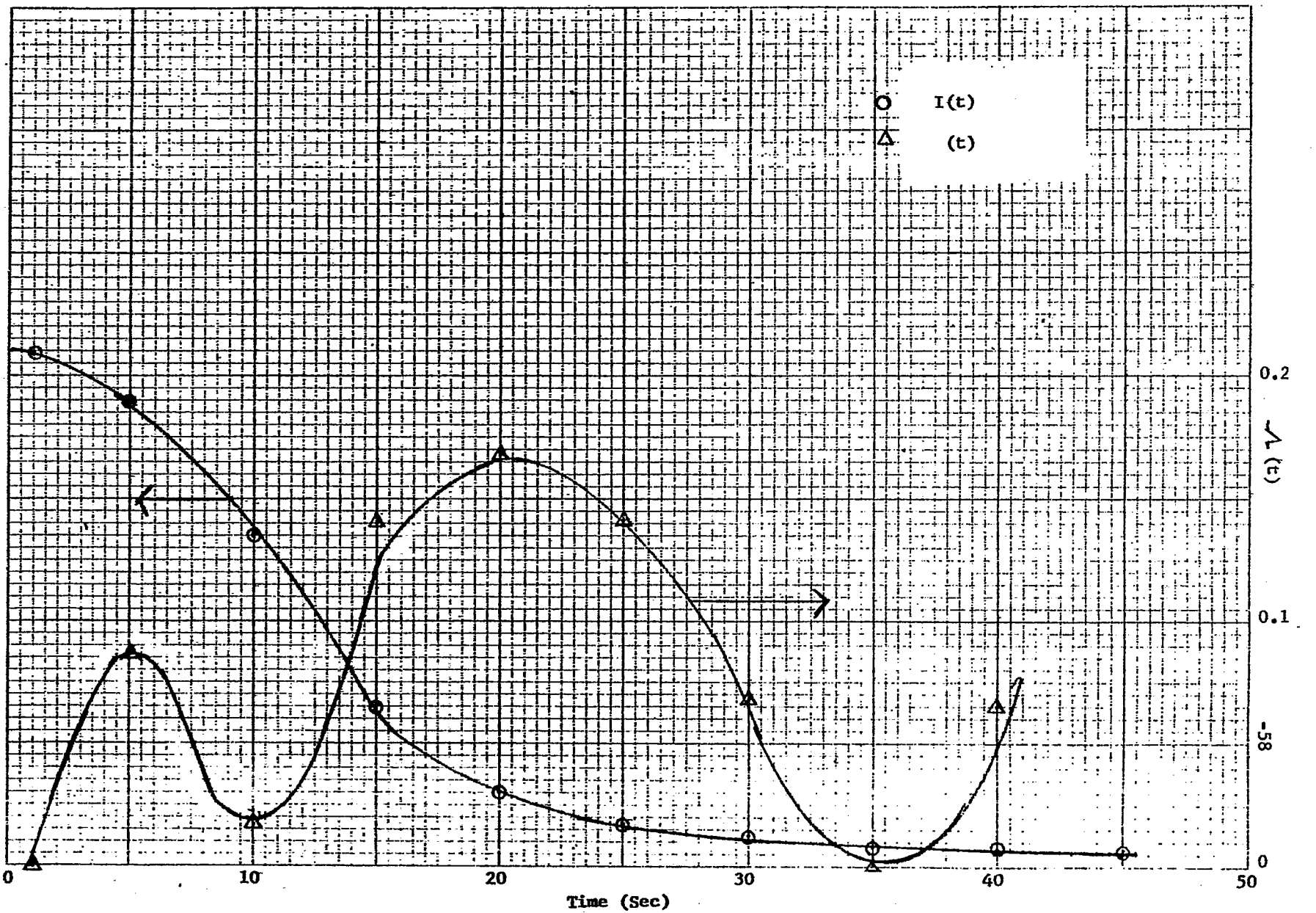

U.S. DEPARTMENT OF COMMERCE
Technology Administration
National Technical Information Service
Springfield, VA 22161 (703) 605-6000